Inorganic Chemistry

Article

pubs.acs.org/IC

Influence of Crown Thioether Ligands in the Structures and of Perhalophenyl Groups in the Optical Properties of Complexes with Argentoaurophilic Interactions

Alexander J. Blake,[†] Rocío Donamaría,[‡] Vito Lippolis,*[,§] José M. López-de-Luzuriaga,*[,‡] Elena Manso,[‡] Miguel Monge,[‡] and M. Elena Olmos*[,‡]

[†]School of Chemistry, The University of Nottingham, University Park, Nottingham NG7 2RD, U.K.

[‡]Departamento de Química, Centro de Investigación de Síntesis Química (CISQ), Complejo Científico-Tecnológico, Universidad de La Rioja, Madre de Dios 51 26004 Logroño, Spain

[§]Dipartimento di Scienze Chimiche e Geologiche, Università degli Studi di Cagliari, S.S. 554 Bivio per Sestu, 09042 Monserrato, Cagliari, Italy

Supporting Information

ABSTRACT: Reaction of $[\{Au(C_6X_5)_2\}Ag]_n$ (X = Cl, F) with the crown thioethers 1,4,7-trithiacyclononane ([9]aneS$_3$), 1,4,8,11-tetrathiacyclotetradecane ([14]aneS$_4$), or 1,4,7,10,13,16,19,22-octathiacyclotetracosane ([24]aneS$_8$) affords a series of heteronuclear Au^I/Ag^I compounds of stoichiometry $[\{Au(C_6X_5)_2\}Ag(L)_x]$ (L = [9]aneS$_3$, x = 2 (**1**, **4**); L = [14]aneS$_4$, x = 1 (**2**, **5**); L = [24]aneS$_8$, x = 0.5 (**3**, **6**)) formed via Ag−S bonds and Au···Ag contacts. X-ray diffraction studies of some of these complexes reveal different structural arrangements and nuclearity depending on the nature of the crown thioether ligand and on the presence or absence of aurophilic interactions. All the complexes are luminescent in the solid state but not in solution. Density functional theory calculations on representative model systems of complexes **2**−**4** and **6** were carried out to determine the origin of the electronic transitions responsible for their optical properties, which strongly depend on the nature of the perhalophenyl groups bonded to gold.

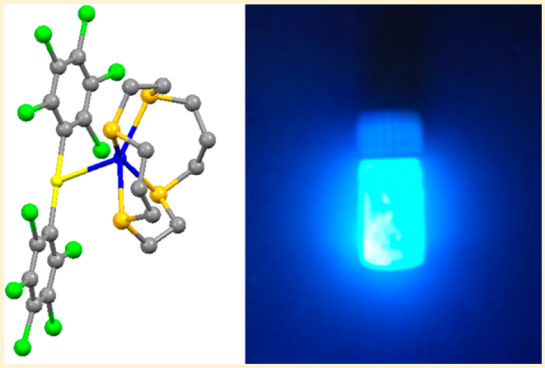

INTRODUCTION

As has been well-established, heavy atoms tend to form polynuclear aggregates with metal···metal interactions displaying distances shorter than the sum of their van der Waals radii. In the case of closed-shell metals, this fact has been related mainly to correlation effects reinforced by relativistic ones, which are a minor component of the interaction-energy stabilization.[1] In the case of gold, numerous examples of homoatomic associations through aurophilic contacts have been described,[2] but the term aurophilicity has nowadays been extended to the wider concept of metallophilicity, since gold complexes displaying interactions with other closed-shell metal ions, such as Cu(I),[3] Ag(I),[3b] Tl(I),[3c,4] Pb(II),[4b] Hg(II),[5] Bi(III),[6] or Sn(II),[7] have been reported, and theoretical studies of selected examples have been carried out. The synthesis of new species showing anomalous structural situations or the nonfulfillment of Coulomb's Law has been possible thanks to the presence of these secondary interactions.[8] Such complexes display structures involving a large variety of assemblies based on metallophilicity, which lead to structural arrangements that vary from discrete molecules[6,7,9] to extended linear chains mediated by gold···gold or gold···heterometal interactions,[3d,4a,b,d,5a,10] or even to two- or three-dimensional arrays.[10d,11] In terms of the properties of these types of compounds, their photophysical properties could be emphasized, and, in particular, their luminescence seems to be closely related to the presence of metal···metal interactions.[12] Moreover, the structural arrangement of the metals, their environment, and the nature of the ligands present in the complex have a strong influence on the luminescent behavior of the complexes.[11a,13]

In recent years we have used basic aurate(I) anions, such as $[AuR_2]^-$ (R = C_6F_5, $C_6F_3Cl_2$ or C_6Cl_5), which react with metal salts acting as Lewis acids, allowing us to synthesize complexes featuring unsupported Au(I)···M interactions [M = Ag(I),[3b,10b,14] Cu(I),[9c,15] Tl(I)[9d,10a,16] and Bi(III)[6]]. For example, the synthesis of polymeric Au/Ag materials of the type $[Au_2Ag_2(C_6F_5)_4L_2]_n$ (L = neutral ligand) by reaction of $[NBu_4][Au(C_6F_5)_2]$ with silver salts was reported more than 20 years ago,[17] although until the beginning of this century their optical properties and potential applications had not been studied. Their solid-state structures, consisting of tetranuclear Ag_2Au_2 units linked via unsupported Au···Au contacts, make

Received: June 28, 2014
Published: September 12, 2014

Scheme 1. Synthesis of Compounds 1−6

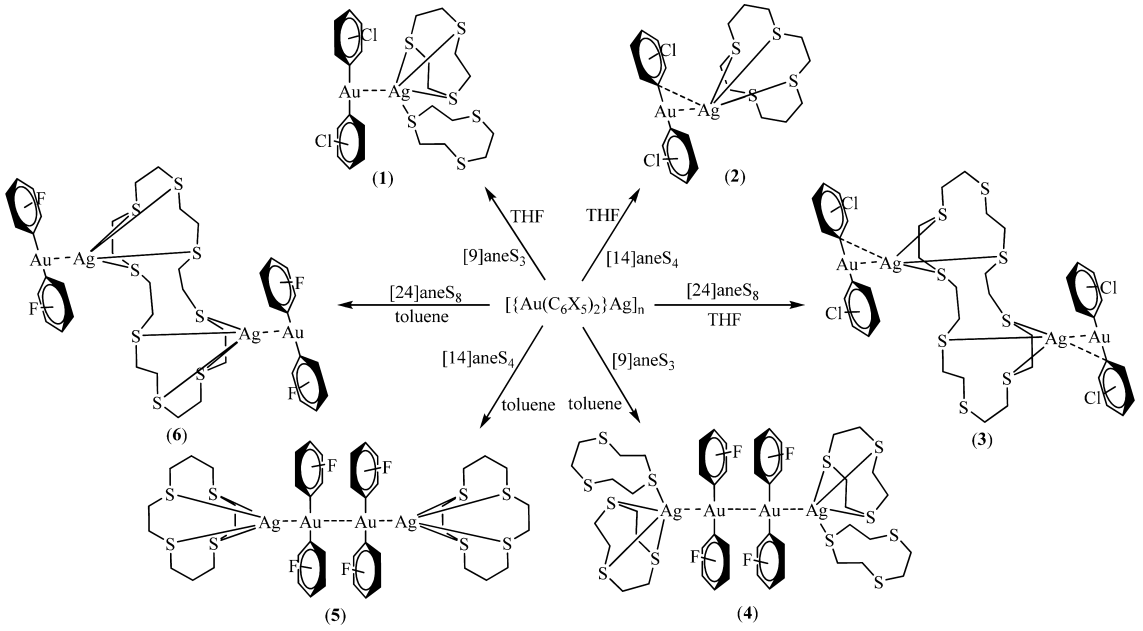

them very interesting from a photophysical point of view since their optical properties are strongly affected by the presence of small organic molecules and can even act as volatile organic compounds sensors.[14]

On the other hand, crown thioethers with a variety of numbers of S-donor atoms have been useful in the synthesis of many coordination compounds featuring a diversity of metal centers.[18] Such ligands can form stable and inert compounds with a great variety of transition metal ions, in which the metal center is sometimes forced to adopt uncommon coordination geometries and/or oxidation states.[19] A detailed inspection of the coordination chemistry of p-block[20] and d^{10} transition metal ions[21] with crown thioethers is still an open area of research and include some silver(I) complexes with crown thioethers that have been structurally characterized, such as $[Ag([9]aneS_3)_2]I_5$[22] and $[Ag_2([24]aneS_8)(CF_3SO_3)_2(MeCN)_2]_\infty$.[23] In the crystal structure of the cation $[Ag([9]aneS_3)_2]^+$ two $[9]aneS_3$ molecules are facially bound to the silver(I) center imposing an octahedral coordination environment to the metal. In addition, the unusual trinuclear silver(I) complex cation $[Ag_3([9]aneS_3)_3]^{3+}$ incorporates bridging thioether ligands, and the metal ions exhibit a highly distorted tetrahedral coordination environment provided by four S donors.[24] The complex $[Ag_2([24]aneS_8)(CF_3SO_3)_2(MeCN)_2]_\infty$ also shows each Ag(I) center coordinated to four S-donor atoms from two different ligand molecules in a distorted tetrahedral environment, with a disposition of both silver(I) ions and macrocycles acting as bridging ligands and thereby forming an extended ladder.[23]

Taking all the above into account, we decided to study the reactivity of the basic precursors $[Au(C_6X_5)_2]^-$ (X = Cl, F) toward $Ag(OClO_3)$, which acts as an acid, in the presence of S-donor polydentate ligands, such as 1,4,7-trithiacyclononane ($[9]aneS_3$), 1,4,8,11-tetrathiacyclotetradecane ($[14]aneS_4$), and 1,4,7,10,13,16,19,22-octathiacyclotetracosane ($[24]aneS_8$). The influence of the macrocyclic ligand employed in these reactions is evident, since they lead to complexes with a different content of neutral ligand (2, 1, or 0.5 molecules of thioether per silver center) when $[9]aneS_3$, $[14]aneS_4$ or $[24]aneS_8$, respectively, are used.

SYNTHESIS AND CHARACTERIZATION

We have studied the reactivity of basic gold(I) species of the type $[Au(C_6X_5)_2]^-$ (X = Cl, F) with acid silver(I) salts in the presence of S-donor polydentate ligands, such as $[9]aneS_3$, $[14]aneS_4$, or $[24]aneS_8$. The modifications in the aryl group and/or in the S-donor ligand influence both the number of intermetallic interactions and their strength, and consequently, compounds with different solid state structures and optical properties are obtained.

By reaction of the polymetallic chain compound $[\{Au(C_6Cl_5)_2\}Ag]_n$ in the appropriate molar ratio with the crown thioether $[9]aneS_3$, $[14]aneS_4$, or $[24]aneS_8$ in tetrahydrofuran (THF), the heteronuclear gold/silver complexes $[\{Au(C_6Cl_5)_2\}Ag([9]aneS_3)_2]$ (**1**), $[\{Au(C_6Cl_5)_2\}Ag([14]aneS_4)]$ (**2**), or $[\{Au(C_6Cl_5)_2\}_2Ag_2([24]aneS_8)]$ (**3**) are obtained in good yields as yellow (**1**) or white (**2**, **3**) solids (see Scheme 1). The substitution of the chlorine atoms of the aryl groups by fluorine does not affect the stoichiometry of the resulting compounds, and so, regardless of the molar ratio of the starting products, the species $[\{Au(C_6F_5)_2\}Ag([9]aneS_3)_2]_2$ (**4**), $[\{Au(C_6F_5)_2\}Ag([14]aneS_4)]_2$ (**5**), or $[\{Au(C_6F_5)_2\}_2Ag_2([24]aneS_8)]$ (**6**) are obtained as white solids when $[\{Au(C_6F_5)_2\}Ag]_n$ is treated with the corresponding macrocyclic ligand in toluene. Although the synthesis of complexes **4**−**6** can also be carried out in THF, the use of toluene leads to higher yields. However, toluene cannot be employed as a solvent in the synthesis of compounds **1**−**3** since the metallic precursor $[\{Au(C_6Cl_5)_2\}Ag]_n$ is insoluble in it. All the complexes are stable to air and moisture for long periods of time at room temperature. Complexes **1** and **4**−**6** are soluble in O-donor solvents, such as THF or acetone, partially soluble in dichloromethane or acetonitrile, and insoluble in hexane or diethyl ether, while **2** and **3** are nearly insoluble in all the solvents we tested. Their elemental analyses and spectroscopic data are in accordance with the proposed stoichiometry (see Experimental Section).

dx.doi.org/10.1021/ic501515c | Inorg. Chem. 2014, 53, 10471−10484

Table 1. Data Collection and Structure Refinement Details for Complexes 2, 3, 4, and 6

compound	2	3	4	6
chemical formula	$C_{22}H_{20}AgAuCl_{10}S_4$	$C_{40}H_{32}Ag_2Au_2Cl_{20}S_8$	$C_{24}H_{24}AgAuF_{10}S_6$	$C_{40}H_{32}Ag_2Au_2F_{20}S_8$
crystal habit	colorless plate	colorless prism	colorless plate	colorless prism
crystal size/mm	0.20 × 0.07 × 0.005	0.15 × 0.10 × 0.07	0.59 × 0.56 × 0.07	0.45 × 0.15 × 0.08
crystal system	monoclinic	triclinic	monoclinic	triclinic
space group	$P2_1/n$	$P\bar{1}$	$P2_1/c$	$P\bar{1}$
a /Å	8.4456(5)	10.5243(8)	14.8817(6)	9.7697(6)
b /Å	21.8643(12)	10.6311(7)	11.4985(5)	10.3420(6)
c /Å	17.2493(5)	14.3009(11)	18.8685(7)	13.2998(8)
α /deg	90	73.651(3)	90	69.799(3)
β/deg	92.410(3)	85.776(3)	112.542(2)	80.194(3)
γ/deg	90	71.819(4)	90	72.771(3)
U /Å^3	3182.4(3)	1458.53(18)	2982.0(2)	1201.07(12)
Z	4	1	4	1
D_c /g cm^{-3}	2.237	2.377	2.227	2.432
M	1071.96	2087.81	999.63	1758.81
$F(000)$	2048	992	1920	832
T /°C	−90	−100	−123	−103
$2\theta_{max}$/deg	55	55	55	55
μ(Mo Kα)/mm^{-1}	6.339	6.912	6.071	7.351
no. of reflections measured	44 974	22 114	36 415	17 117
no. of unique reflections	7203	6668	6824	5483
R_{int}	0.0921	0.074	0.0371	0.0511
R^a ($I > 2\sigma(I)$)	0.0477	0.0452	0.0321	0.0326
wR^b (F^2, all refl.)	0.1036	0.0924	0.0829	0.0870
no. of parameters	343	325	433	325
no. of restraints	0	0	530	74
S^c	1.116	1.052	0.998	1.055
max. $\Delta\rho$/eÅ^{-3}	3.212	3.497	4.461	3.846

$^a R(F) = \Sigma \, ||F_o| - |F_c|| / \Sigma \, |F_o|$. $^b wR(F^2) = [\Sigma \{w(F_o^2 - F_c^2)^2\} / \Sigma \{w(F_o^2)^2\}]^{0.5}$; $w^{-1} = \sigma^2(F_o^2) + (aP)^2 + bP$, where $P = [F_o^2 + 2F_c^2]/3$ and a and b are constants adjusted by the program. $^c S = [\Sigma \{w(F_o^2 - F_c^2)^2\}/(n-p)]^{0.5}$, where n is the number of data and p the number of parameters.

The presence of the perhalophenyl groups bonded to gold(I) is evident from their IR spectra, which show, among others, absorptions due to the C_6Cl_5 or C_6F_5 ligands at 614 and 834 cm^{-1} (**1**–**3**) or at ∼1505, ∼955 and ∼785 cm^{-1} (**4**–**6**). On the other hand, the conductivity measurements of solutions of **1** and **4**–**6** in acetone are in accordance with a ionic formulation of the complexes, since they behave as 1:1 (**1**, **4** and **5**) or 2:1 electrolytes (**6**), which suggests dissociation in solution into $[Au(C_6X_5)_2]^-$ anions and $[Ag([9]aneS_3)_2]^+$ (**1** and **4**) $[Ag([14]aneS_4)]^+$ (**5**) or $[Ag_2([24]aneS_8)]^{2+}$ (**6**) cations. The low solubility of complexes **2** and **3** precluded measurement of their molar conductivity in solution. These results agree with our previous observations on related Au/Tl compounds[25] or on other complexes obtained through acid–base reactions of the metalloligand $[Au(C_6X_5)_2]^-$ with an heterometal, in which dissociation into their ionic counterparts is observed in solution.

The ^{19}F NMR spectra of **4**–**6** in [D$_8$]-THF resembles that of the precursor complex $NBu_4[Au(C_6F_5)_2]$, showing the characteristic pattern and chemical shifts of pentafluorophenylgold(I) derivatives (see Experimental Section). Because of the low solubility of **2** and **3** in common solvents, their ^{1}H NMR spectra were recorded in [D$_6$]-dimethyl sulfoxide, while all other ^{1}H NMR spectra were recorded in [D$_8$]-THF. The coordination of the macrocyclic ligands to silver is evident in the ^{1}H NMR spectra of **1**–**6**, in which the resonances due to the protons of these ligands appear slightly shifted relative to those observed in the spectra of the free ligands. Thus, all the protons of 1,4,7-trithiacyclononane ([9]aneS$_3$) appear as a singlet at 2.92 (**1**) or 3.01 ppm (**4**), while in the spectrum of free [9]aneS$_3$ in the same solvent the signal is located at 3.21 ppm. In the case of 1,4,8,11-tetrathiacyclotetradecane ([14]aneS$_4$), its ^{1}H NMR spectrum displays three signals at 2.02 (*q*, S−CH$_2$−CH$_2$−CH$_2$−S), 2.74 (*t*, S−CH$_2$−CH$_2$−CH$_2$−S), and 2.86 ppm (*s*, S−CH$_2$−CH$_2$−S) with a relative integration 1:2:2, resonances that appear at 1.86, 2.68, and 2.79 ppm in the spectrum of complex **2** or at 2.03, 2.85, and 2.87 ppm in the case of **5**. Finally, the singlet due to the equivalent hydrogen atoms of 1,4,7,10,13,16,19,22-octathiacyclotetracosane ([24]aneS$_8$) is located at 2.92 ppm in the spectrum of the free ligand, and it shifts to 2.90 (**3**) or to 3.08 ppm (**6**) as a consequence of the coordination of its sulfur atoms to silver(I).

In the mass spectra (MALDI−) of the new products the base peak corresponding to the aurate(I) anion $[Au(C_6X_5)_2]^-$ is observed at m/z = 695 (**1**–**3**) or 531 (**4**–**6**). Their MALDI+ mass spectra display a base peak corresponding to the fragment $[Ag(L)_2]^+$ at m/z = 469 (**1** and **4**) or to$[Ag(L)]^+$ at m/z = 377 (**2** and **5**) or 589 (**3** and **6**), confirming the coordination of the S-donors silver centers, but no other fragment of higher dimensionality is detected, which also is in accordance with a dissociative process in solution. In all of them the experimental isotopic distributions are in agreement with the calculated ones.

CRYSTAL STRUCUTURES

The crystal structures of complexes **2**–**6** were established by X-ray diffraction studies from single crystals grown by a variety of procedures. For complexes **2** and **3** crystals were obtained by

dx.doi.org/10.1021/ic501515c | Inorg. Chem. 2014, 53, 10471−10484

slow diffusion of a solution of the crown thioether ligand in diethyl ether into a solution of the precursor $[\{Au(C_6Cl_5)_2\}-Ag]_n$ in THF (**2**) or butyronitrile (**3**). Other single crystals were obtained by slow diffusion of *n*-hexane into a saturated solution of complex **4** in THF, by slow diffusion of diethyl ether into a solution of **6** in butyronitrile or by slow evaporation of the solvent from a THF solution of complex **5**. Details of the data collection and refinement are given in Table 1, and selected bond lengths and angles appear in Tables 2−5. Because of the low quality of the available crystals of **5**, no publishable results could be obtained, although there is no doubt about the overall molecular structure and the disposition of ligands and metals. The structure consists of a tetranuclear species formed by two $[Ag([14]aneS_4)]^+$ units, with the crown thioethers acting as tetradentate ligands and two linear $[Au(C_6F_5)_2]^-$ fragments linked through unsupported metal···metal interactions with an alternating Ag−Au−Au−Ag sequence of metals.

The crystal structures of **2**−**6** resemble those recently described by us for the related Au/Tl derivatives containing the same macrocycles,[25] since they all contain $[Au(C_6X_5)_2]^-$ units connected to the silver(I) atom of the cationic $[Ag(L)_x]^+$ (x = 2, 1, 0.5) fragments via unsupported Au···Ag interactions. Thus, in all of them the gold(I) centers of the bis(aryl)aurate(I) units are linearly coordinated (the maximum deviation from linearity for the C−Au−C angle of 2.25° occurs in **6**) to two perhalophenyl groups, showing typical Au−C distances that range from 2.037(5) (**6**) to 2.069(7) Å (**3**). Nevertheless, there are differences between them, not only due to the nature of the S-donor ligand bonded to silver but also because of the nature of the halogens present in the aryl groups bonded to gold(I), which influence the presence or absence of Ag···C_{ipso} interactions as well as the Au−Ag distances.

It is noteworthy that complex **2** represents the first example of a dinuclear Au/Ag compound displaying an unsupported Au···Ag contact, given that in the three heterodinuclear Au/Ag products with a metallophilic interaction described previously there is at least one bridging ligand assisting such a contact.[3b,26] Moreover, apart from $\{[(Tab)_2Ag][Au(CN)_2]\}_2$ (Tab = 4-(trimethylammonio)benzenethiolate),[9a] complexes **4** and **5** are the only discrete molecules in which a linear or pseudolinear Ag−Au−Au−Ag disposition of the metal centers is observed.

The ring size of the crown thioether is the structural factor determining its behavior as terminal or bridging ligand. Hence, the crystal structures of **2** and **4** contain one $[14]aneS_4$ and two $[9]aneS_3$ macrocycles, respectively, coordinated to silver(I) as terminal ligands through four sulfur atoms (Figure 1), although with different strength according to the Ag−S distances observed. Thus, while in the pentachlorophenyl derivative **2** the Ag−S distances vary from 2.640(2) to 2.740(2) Å, the pentafluorophenyl complex **4** displays one weaker [2.8907(11) Å] and three stronger [2.4727(10)−2.5965(11) Å] Ag−S bonds. All these values lie within the range of Ag−S distances described for other silver(I) derivatives containing the same macrocyclic ligands,[21c,22,24,27] in which the Ag−S lengths vary from 2.443(2) Å in $[Ag([9]aneS_3)]_4(CF_3SO_3)_4\cdot 2MeNO_2$[27b] to 2.777(2) Å in $[Ag([9]aneS_3)_2]I_5$[22] and from 2.4655(13) to 3.0199(13) Å in $[Ag_2(Fod)_2([14]aneS_4)]_\infty$ (H-Fod = 2,2-dimethyl-6,6,7,7,8,8,8-heptafluoro-3,5-octanedione).[27a] In addition, both crystal structures present argentoaurophilic inter-

Table 2. Selected Bond Lengths [Å] and Angles [deg] for Complex 2

Ag−Au	2.8200(6)	Ag−S(2)	2.676(2)
Au−C(1)	2.053(6)	Ag−S(3)	2.675(2)
Au−C(11)	2.055(7)	Ag−S(4)	2.740(2)
Ag−S(1)	2.640(2)	Ag−C(1)	2.900(6)
C(1)−Au−C(11)	179.6(3)	S(2)−Ag−S(4)	147.65(6)
S(1)−Ag−S(3)	148.78(7)	S(1)−Ag−Au	92.31(5)
S(1)−Ag−S(2)	97.31(6)	S(3)−Ag−Au	114.20(5)
S(3)−Ag−S(2)	81.24(6)	S(2)−Ag−Au	125.05(5)
S(1)−Ag−S(4)	80.80(6)	S(4)−Ag−Au	87.27(4)
S(3)−Ag−S(4)	84.16(6)		

Table 3. Selected Bond Lengths [Å] and Angles [deg] for Complex 3

Au−Ag	2.8077(6)	Ag−S(1)	2.6254(19)
Au−C(1)	2.061(6)	Ag−S(2)	2.648(2)
Au−C(11)	2.069(7)	Ag−C(1)	2.695(6)
Ag−S(4)	2.5419(18)		
C(1)−Au−C(11)	178.6(3)	S(2)−Ag−C(1)	95.88(15)
S(4)−Ag−S(1)	138.43(6)	S(4)−Ag−Au	101.83(4)
S(4)−Ag−S(2)	116.51(6)	S(1)−Ag−Au	91.89(4)
S(1)−Ag−S(2)	79.90(6)	S(2)−Ag−Au	130.53(4)
S(1)−Ag−C(1)	114.60(14)	C(1)−Ag−Au	43.94(13)
S(4)−Ag−C(1)	101.96(14)		

Table 5. Selected Bond Lengths [Å] and Angles [deg] for Complex 6

Au−Ag	2.8583(4)	Ag−S(1)	2.5881(12)
Au−Au#1[a]	3.5580(3)	Ag−S(2)	2.7231(13)
Au−C(1)	2.037(5)	Ag−S(3)	2.8800(15)
Au−C(11)	2.042(4)	Ag−S(4)	2.5900(12)
C(1)−Au−C(11)	177.75(18)	S(2)−Ag−Au	94.39(3)
S(1)−Ag−S(4)	130.31(4)	S(1)−Ag−S(3)	90.78(4)
S(1)−Ag−S(2)	83.44(4)	S(4)−Ag−S(3)	78.70(4)
S(4)−Ag−S(2)	137.63(4)	S(2)−Ag−S(3)	75.76(4)
S(1)−Ag−Au	117.84(3)	Au−Ag−S(3)	148.81(3)
S(4)−Ag−Au	90.30(3)		

[a]Symmetry transformations used to generate equivalent atoms: #1 = $-x + 2, -y + 1, -z + 1$.

Table 4. Selected Bond Lengths [Å] and Angles [deg] for Complex 4

Au(1)−C(7P)	2.047(5)	Ag(1)−S(11)	2.4727(10)
Au(1)−C(1P)	2.048(5)	Ag(1)−S(4)	2.5612(10)
Au(1)−Ag(1)	3.0763(4)	Ag(1)−S(7)	2.5965(11)
Au(1)−Au(1)#1[a]	3.3702(3)	Ag(1)−S(1)	2.8907(11)
C(7P)−Au(1)−C(1P)	177.83(16)	S(11)−Ag(1)−S(7)	136.71(4)
Ag(1)−Au(1)−Au(1)#1[a]	160.879(11)	S(4)−Ag(1)−S(7)	86.11(4)
S(11)−Ag(1)−S(4)	136.99(4)	S(1)−Ag(1)−Au(1)	166.39(2)

[a]Symmetry transformations used to generate equivalent atoms: #1 = $-x + 1, -y, -z + 1$.

dx.doi.org/10.1021/ic501515c | Inorg. Chem. 2014, 53, 10471−10484

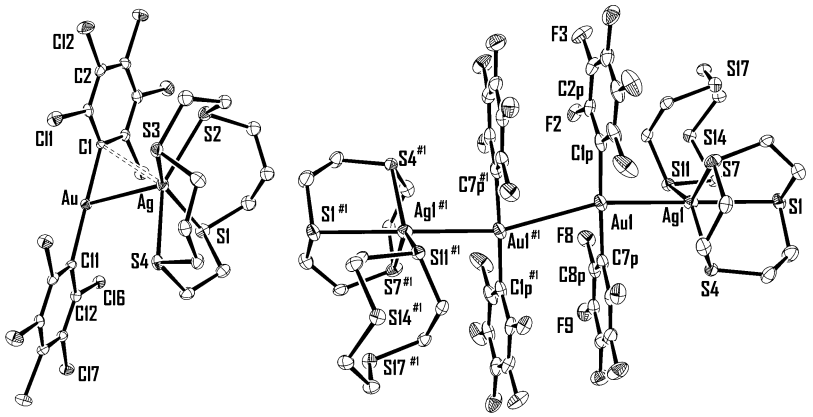

Figure 1. Molecular structures of **2** (left) and **4** (right) with the labeling scheme for the atoms positions. Hydrogen atoms are omitted for clarity, and ellipsoids are drawn at the 30% level. #1 = $-x + 1, -y, -z + 1$.

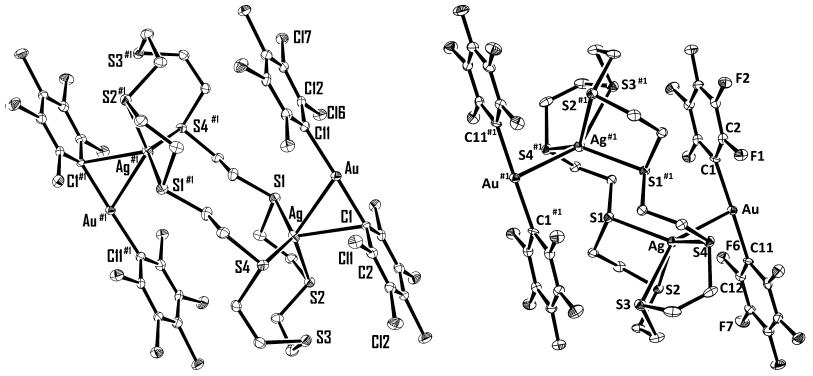

Figure 2. Molecular structures of **3** (left) and **6** (right) with the labeling scheme for the atoms positions. Hydrogen atoms are omitted for clarity, and ellipsoids are drawn at the 30% level. #1 = $-x + 2, -y + 1, -z + 1$ (**3**); #1 = $-x + 1, -y + 2, -z + 1$ (**6**).

actions that lead to a coordination number of five for silver(I): **2** exhibits a distorted square-based pyramidal environment with the gold(I) at the vertex, while the distorted trigonal bipyramidal environment in **4** has Au1 and S1 in the apical positions (see Figure 1).

The silver(I) center in complex **2** participates in a weak Ag···C contact of 2.900(6) Å with the *ipso* carbon atom of one of the perfluoroaryl rings bonded to gold(I). This contact is longer than those reported for other complexes containing $[Au(C_6X_5)_2]^-$ units interacting with silver(I) through both Au···Ag and Ag···C_{ipso} contacts, in which Ag···C distances lie in the range of 2.4396(6)−2.687(6) Å.[3d,9a,10b,14,28] The Ag··C_{ipso} interaction in **2** is probably the reason for the shortness of the Au···Ag distance of 2.8200(6) Å in this complex relative to that in **4**, 3.0763(4) Å. The former is nearly identical to those described in $[(pyPPh_2)_2AuAg(OClO_3)_2]$[26a] [2.820(1) Å], $[\{(Ph_3P)Au(\mu\text{-mes})Ag(SC_4H_8)\}_2][SO_3CF_3]_2$ (mes = 2,4,6-$C_6H_2Me_3$) [2.8245(6) Å],[29] or $[AuAg_4(mes)(CF_3CO_2)_4(tht)]_n$ [2.8226(4) Å],[11c] all of them containing bridging $pyPPh_2$ or mesityl ligands, with Ag···C_{ipso} distances in the latter two of 2.326(3),[29] 2.530(4), and 2.614(4) Å.[11c] In contrast, the Au···Ag distance in **4** is one of the longest reported to date and only comparable to one of the Au···Ag distances in $[AuAg_4(mes)(CF_3CF_2CO_2)_4(tht)]_n$ [3.0782(6) Å],[11c] in which the Ag···C_{ipso} distances are 2.385(6) and 2.588(6) Å. Apart from the presence of a Ag···C_{ipso} contact in **2**, which is absent in **4**, there is an important difference between these crystal structures, since only the latter displays an aurophilic interaction, thus leading to a discrete tetranuclear molecule with a pseudolinear L_2−Ag−Au−Au−Ag−L_2 arrangement of ligands and metals (Figure 1), the same as that observed in the crystal structure of **5**.

As noted above, [14]aneS_4 and [9]aneS_3 act as terminal ligands in complexes **2** and **4**, respectively, while in complexes **3** and **6** [24]aneS_8 bridges two Ag(I) centers. Therefore, the increasing number of sulfur centers in the crown thioether, and hence the size of the macrocyclic ring, does control the behavior of the S-donor ligand. In the crystal structures of **3** and **6** we observe the same Au−Ag−L−Ag−Au sequence (Figure 2) found in the related Au/Tl complexes $[\{Au(C_6Cl_5)_2\}_2Tl_2([24]aneS_8)]_n$ and $[\{Au(C_6F_5)_2\}_2Tl_2([24]aneS_8)]$,[25] although none of the Au/Ag derivatives display the aurophilic interactions that are the responsible for the polymeric nature of the pentachlorophenyl Au/Tl compound.

Again, the nature of the halogen atoms present in the aryl groups appears to play an important role in the Ag···C_{ipso} interactions as well as in the Au···Ag distances, since the former are again present in the pentachlorophenyl derivative **3**, whereas they are not observed in the pentafluorophenyl complex **6**, similar to what occurs in **2** and **4**. As in compound **2**, the Ag···C_{ipso} distance in **3** [2.695(6) Å] is longer than those described for other Au/Ag compounds with bis(aryl)aurate(I) units showing Au···Ag and Ag···C_{ipso} interactions, where the Ag···C_{ipso} distances range from 2.4396(6) to 2.687(6) Å,[3d,9a,10b,14,28] although it is considerably shorter than in complex **2** [2.900(6) Å]. This stronger interaction is also accompanied by a reinforcement of the argentoaurophilic contact, which is evidenced by the fact that the Au···Ag separation in **3** [2.8077(6) Å] is the shortest one described in

dx.doi.org/10.1021/ic501515c | *Inorg. Chem.* 2014, 53, 10471−10484

this paper (see Table 3); however, it is longer than those found in the polymeric species $[Au_2Ag_2R_4L_2]_n$ (R = perhalophenyl group, L = neutral ligand), in which the Au···Ag distances lie in the range of 2.7003(4)−2.792(2) Å.[3d,9a,10b,14,17,28] In summary, the pentachlorophenyl complexes **2** and **3** show Ag···C_{ipso} interactions, which are absent in the pentafluorophenyl compounds **4** and **6**, as well as stronger Au···Ag contacts, whose strengths increase simultaneously with the former interactions.

Finally, although both **3** and **6** contain [24]aneS$_8$ as bridging ligand, there is a difference probably related to the Ag···C contacts described above: in **3**, where this interaction is observed and it is stronger than in **2**, only three of the sulfur atoms of the macrocycle bind to the silver, while in **6** there is a fourth Ag−S bond, thus leading to pentacoordinated silver(I)-centers in both crystal structures. The environment of silver could be described as distorted square-based pyramidal with C1 (**3**) or S1 (**6**) at the vertex [τ = 0.13 (**3**), 0.19 (**6**)].[30] The Ag−S bond lengths in **3** range from 2.5419(18) to 2.648(2) Å, whereas in **6** they vary over a wider range, displaying two shorter [2.5881(12) and 2.5900(12) Å] and two longer [2.7231(13) and 2.8800(15) Å] Ag−S distances. A similar situation is observed in $[Ag_2([24]aneS_8)(CF_3SO_3)_2(MeCN)_2]_\infty$, with values between 2.5400(14) and 2.627(2) Å,[23] and in $[Ag_2([24]aneS_8)](NO_3)_2$, where Ag−S distances lie in the range of 2.4921(11)−2.8932(12) Å.[23]

PHOTOPHYSICAL PROPERTIES

Absorption in Solution. The absorption spectra of complexes **1** and **4**−**6** show similar features to those described for the related gold(I)−thallium(I) derivatives reported previously by some of us.[25] Thus, in the case of complex **1** it displays two absorptions at 236 and 284 nm in dilute THF solutions; these bands are also present in the spectra of the heterometallic precursor $[\{Au(C_6Cl_5)_2\}Ag]_n$ and of the gold(I) complex $NBu_4[Au(C_6Cl_5)_2]$ (see Figure 3). It is likely that the

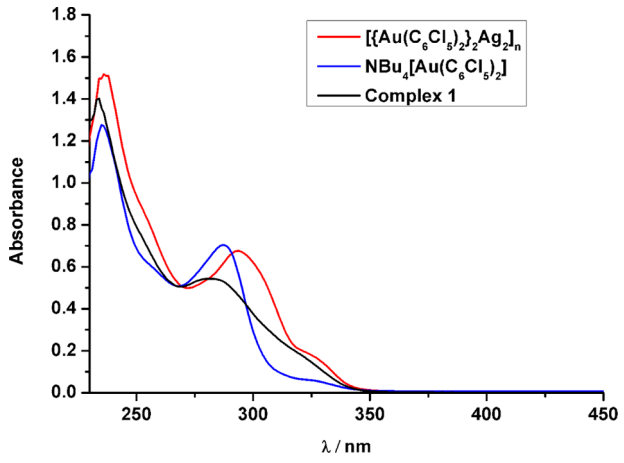

Figure 3. Absorption spectra of complex **1** and the Au(I) and Au(I)−Ag(I) precursors $NBu_4[Au(C_6Cl_5)_2]$ and $[\{Au(C_6Cl_5)_2\}Ag]_n$.

band at high energy arises from transitions between π orbitals in the perhalophenyl groups, while the transitions in the low-energy region probably involve orbitals of the gold centers. Therefore, these absorptions can be assigned to $\pi\rightarrow\pi^*$ and Au$\rightarrow\pi^*$ transitions in the pentachlorophenyl rings. Similar phenomena have been analyzed in detail for gold complexes with aromatic substituents,[31] and we have also done a similar assignment previously for related complexes.[32] Nevertheless, the possibility of an n$\rightarrow\sigma^*$ transition in the thioether ligands for the high-energy absorption cannot be ruled out, since the energy of such transitions has been reported at similar energy values,[33] and the ligands show one absorption at 234 nm, although with less intensity for similar concentrations. In the case of complexes **2** and **3**, also bearing C_6Cl_5 ligands, the absorption spectra in solution could not be recorded due to their low solubility in organic solvents.

For pentafluorophenyl derivatives **4**−**6** the spectra show in all cases similar patterns, displaying three bands at ca. 236, 256, and 280 nm (see Figure 4). In this case the first two bands are

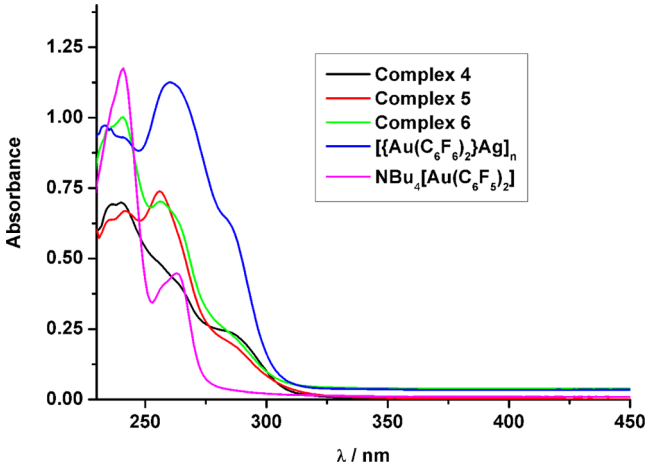

Figure 4. Absorption spectra of complexes **4**−**6** and the Au(I) and Au(I)−Ag(I) precursors $NBu_4[Au(C_6F_5)_2]$ and $[\{Au(C_6F_5)_2\}Ag]_n$.

also present in the gold(I) precursor $NBu_4[Au(C_6F_5)_2]$ and are therefore likely to be due to $\pi\rightarrow\pi^*$ and Au$\rightarrow\pi^*$ transitions in the pentafluorophenyl rings or to an n$\rightarrow\sigma^*$ transition in the thioether ligands for the former. In contrast, the third peak at lower energies does not appear in the spectrum of the gold precursor complex, but it does in that of the heterometallic precursor $[\{Au(C_6F_5)_2\}Ag]_n$. Consequently, this band is tentatively assigned to a transition involving orbitals formed by the interaction between gold(I) and silver(I). In this sense, as we have reported in previous studies, the gold−silver interaction may persist in solution and, among other factors, be responsible for the optical behavior of the complexes that contain it.[34]

Luminescence. The rich structural diversity observed in **1**−**6** leads to a different optical response when the complexes are irradiated with UV light in the solid state. Thus, while complexes **2** and **3** display a strong blue luminescence, complexes **1** (green) and **4**−**6** (blue) are weakly luminescent, both at room temperature and at 77 K (see Table 6 and Figures 5 and 6). None of them are emissive when they are irradiated in solution, probably due to the dissociation of the counterparts in solution, as suggested by the mass spectra and the conductivity measurements; when the solvent is removed by evaporation no degradation of the complexes occurs, and they recover their luminescence. Also, complexes **2** and **3** show lifetimes in the solid state longer than those of complexes **1**, **4**−**6**.

Correlating structural features, metal content, and the type of ligands bonded to the metal centers with the type of emission or its efficiency is not straightforward. Thus, for instance, if we take into account the interactions between the metal centers we

dx.doi.org/10.1021/ic501515c | Inorg. Chem. 2014, 53, 10471−10484

Table 6. Photophysical Properties of Complexes 1−6

complex	UV−vis in THF[a] (nm)	solid (RT) em (exc)	solid (77 K) em (exc)	glass[b] (77 K) em (exc)	τ[c] (ns)	Φ
1	236 (ε = 20 239) 284 (ε = 8212)	509 (364)	503 (335)	492	286.4	10.3
2		450 (273)	433 (321)	442	4800	97.6
3		476 (277)	476 (364)	392	896	82.3
4	236 (ε = 23 281) 256 (ε = 13 200) 280 (ε = 8130)	462 (340)	451 (354)	431	665.8	4.9
5	236 (ε = 11 155) 256 (ε = 12 324) 280 (ε = 3443)	440 (374)	442 (364)	430	307.0	2.2
6	236 (ε = 40 064) 256 (ε = 28 105) 280 (ε = 9703)	444 (368)	446 (340)	426	316.7	3.2

[a] ε is given in $M^{-1}\cdot cm^{-1}$. [b] In butyronitrile (2×10^{-4} M). [c] Solid state at room temperature.

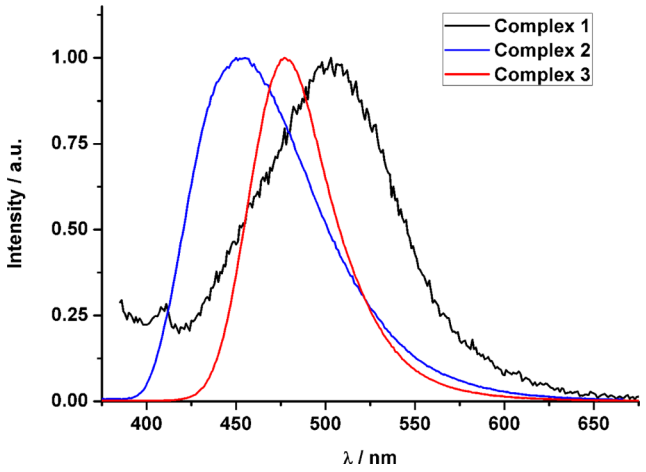

Figure 5. Emission spectra of complexes **1**−**3** in the solid state at room temperature.

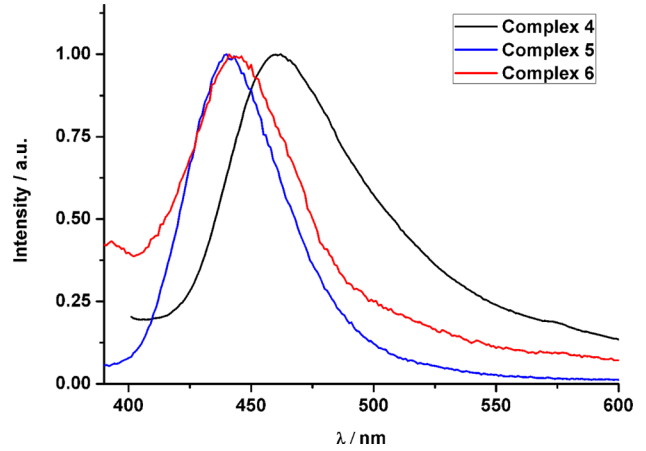

Figure 6. Emission spectra of complexes **4**−**6** in the solid state at room temperature.

observe that, although $Au^I\cdots Au^I$ interactions have been recognized as one of the main origins of the luminescence in many gold(I)-containing complexes,[35] the two complexes displaying stronger luminescence are those in which the gold centers do not interact (**2** and **3**). In addition, one of the strong emitters (complex **3**) shows a Au^I−Au^I distance (3.7195(5) Å) beyond the range of van der Waals interactions (3.32 Å). Besides, $Au^I\cdots Ag^I$ interactions are present in all the structurally characterized complexes, but their strength cannot be considered as the origin of the efficiency of the emissions since, although the pentachlorophenyl derivatives **2** and **3** display shorter $Au^I\cdots Ag^I$ interactions than those of complexes **4** and **6**, within the pentafluorophenyl derivatives complex **5** displays even shorter $Au^I\cdots Ag^I$ contacts (2.761(5) and 2.783(5) Å).

Other aspects that we can consider are the structural disposition of metals and/or ligands. Thus, for instance, complexes **3** and **6** are isostructural; nevertheless, while complex **3** is strongly luminescent, complex **6** is a very weak emitter. In addition, and regarding the number of ligands, in complex **4** there are two [9]aneS$_3$ bonded to each silver atom, while complexes **2** and **5** display one [14]aneS$_4$ bonded to each silver center, and **3** and **6** contain only half of a [24]aneS$_8$ ligand per silver.

Finally, strong luminescence is found in complexes **2** and **3** containing C_6Cl_5 ligands bonded to the gold(I) center, while complexes **4**−**6**, in which the gold atoms are bonded to C_6F_5 ligands, show weak luminescence. Nevertheless, complex **1**, containing pentachlorophenyl rings as ligands, is a weak emitter. At this point it is important to take into account that we have not determined unequivocally the structure of complex **1** by X-ray diffraction studies, and, therefore, its weak luminescence could be due to other factors.

DFT AND TD-DFT CALCULATIONS

As can be seen by the above comments, the assignation of the origin of the luminescence and the justification of the very different emission intensities is puzzling and, therefore, additional tools are needed. For this reason, we carried out density functional theory (DFT) and time-dependent (TD) DFT calculations on model systems representing the solid-state structures for complexes **2**−**4** and **6** (models **2a**−**4a** and **6a**, respectively). This set of model systems permits the study of several parameters that can influence the photophysical properties, such as the C_6Cl_5 or C_6F_5 perhalophenyl groups bonded to gold(I), the crown thioether ligands ([9]aneS$_3$, [14]aneS$_4$, or [24]aneS$_8$) bonded to silver(I), the nuclearity (dinuclear or tetranuclear), or the metal−ligand disposition (see Figure 7). Thus, model **2a** corresponds to the dinuclear complex **2**, representing the $Au^I\cdots Ag^I$ interaction between one $[Au(C_6Cl_5)_2]^-$ anionic fragment and a cationic $[Ag([14]aneS_4)]^+$ one; model **3a** consists of two dinuclear [Au-

dx.doi.org/10.1021/ic501515c | Inorg. Chem. 2014, 53, 10471−10484

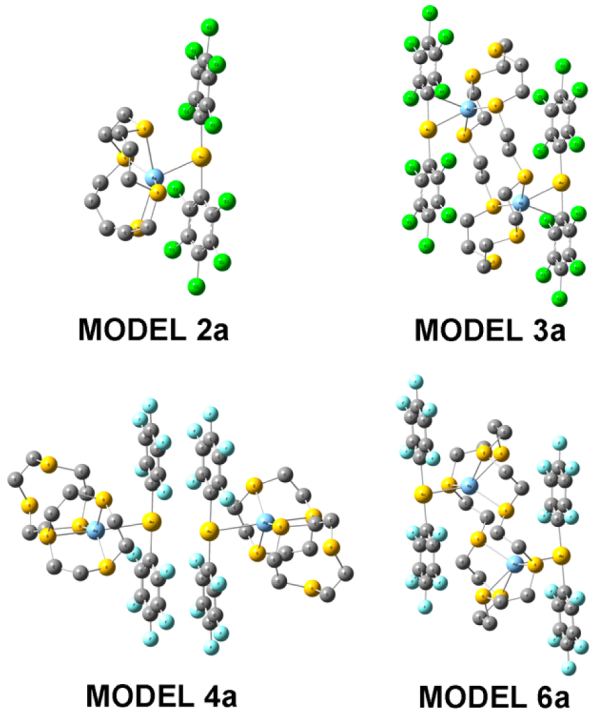

Figure 7. Theoretical model systems $[Au(C_6Cl_5)_2Ag([14]aneS_4)]$ (**2a**), $[Au_2(C_6Cl_5)_4Ag_2([24]aneS_8)]$ (**3a**), $[Au_2(C_6F_5)_4Ag_2([9]aneS_3)_4]$ (**4a**), and $[Au_2(C_6F_5)_4Ag_2([24]aneS_8)]$ (**6a**).

$(C_6Cl_5)_2]^-[Ag]^+$ fragments, bearing one $Au^I\cdots Ag^I$ interaction in each case, bridged through a $[24]aneS_8$ ligand connected to the two silver(I) centers; model **4a** represents an unusual $[Ag]^+-[Au]^-[Au]^-[Ag]^+$ metal disposition with two C_6F_5 ligands bonded to each gold(I) ion and two $[9]aneS_3$ ligands bonded to each silver(I) center; finally, model **6a** is similar to model **3a** but with the C_6Cl_5 ligands replaced by C_6F_5.

We first computed the electronic structures of models **2a**–**4a** and **6a**. Figure 8 and Table 7 display the most important frontier molecular orbitals (MOs) and the population analysis of those MOs, respectively. From these data we can anticipate the contribution of each part of the molecule to the HOMO and LUMO.

In the case of the dinuclear model $[Au(C_6Cl_5)_2Ag([14]aneS_4)]$ (**2a**) the highest occupied MO (HOMO) is mostly located on the $[Ag([14]aneS_4)]^+$ fragment, but HOMO−1 and HOMO−2 are mostly located on the $[Au(C_6Cl_5)_2]^-$ unit; meanwhile, HOMO−3 and HOMO−4 are mostly located on the C_6Cl_5 ligands. In the case of the empty MOs, the lowest unoccupied MO (LUMO) and LUMO+2 are mostly placed on the $[Au(C_6Cl_5)_2]^-$ unit.

Model $[Au_2(C_6Cl_5)_4Ag_2([24]aneS_8)]$ (**3a**) also displays similar features, but in this case the highest occupied MOs from HOMO to HOMO−3 are distributed along the whole molecular arrangement, the contribution from the $[Au(C_6Cl_5)_2]^-$ unit being the highest in all cases. Orbitals LUMO and LUMO+1 are mostly located on the $[Au(C_6Cl_5)_2]^-$ units.

Model $[Au_2(C_6F_5)_4Ag_2([9]aneS_3)_4]$ (**4a**) also shows a high degree of mixing in the contributions from each part of the molecule to the frontier MOs. Nevertheless, it is important to note that the contribution from the $[Ag([9]aneS_3)_2]^+$ fragment is very important both in the HOMOs and the LUMOs, which are the orbitals involved in the most intense theoretical excitations (vide infra).

In the case of model $[Au_2(C_6F_5)_4Ag_2([24]aneS_8)]$ (**6a**), although its structural arrangement is very similar to that of model **3a**, the change of the C_6Cl_5 ligand by a C_6F_5 one affects the overall electronic structure of the molecule. Thus, the

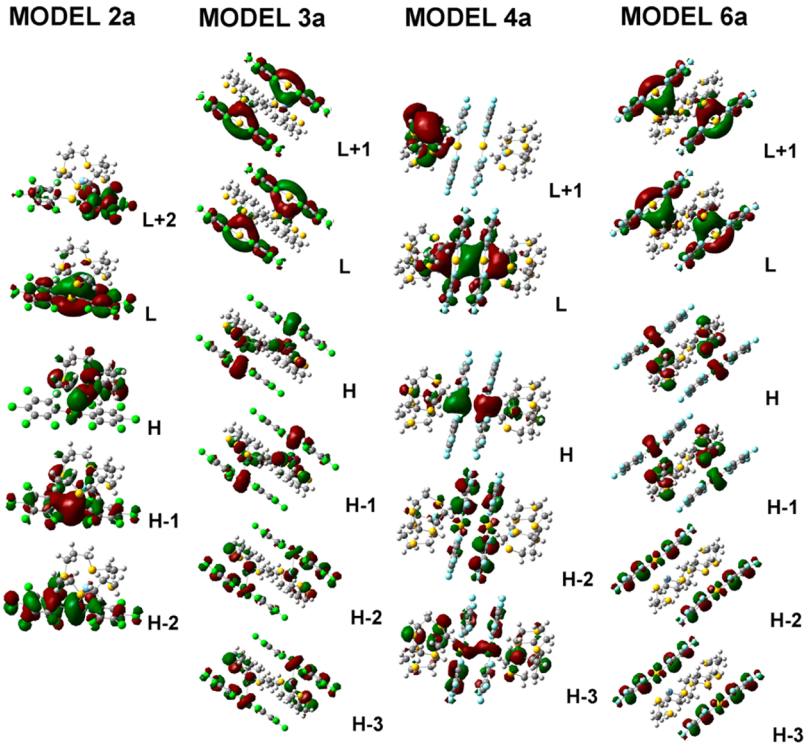

Figure 8. Frontier molecular orbitals (isovalue = 0.02) for model systems **2a**–**4a** and **6a**.

dx.doi.org/10.1021/ic501515c | *Inorg. Chem.* 2014, 53, 10471−10484

Table 7. Population Analysis for Model Systems 2a, 3a, 4a, and 6a

model	orbital[a]	Ag	Au	S-ligand	C_6X_5
2a	LUMO+3	34	39	2	25
	LUMO+2	6	11	3	80
	LUMO+1	63	29	3	5
	LUMO	40	23	7	30
	HOMO	21	5	71	3
	HOMO−1	8	45	15	32
	HOMO−2	1	35	3	61
	HOMO−3	1	4	1	94
	HOMO−4	2	2	2	94
3a	LUMO+1	26	16	13	45
	LUMO	11	14	18	57
	HOMO	19	34	30	17
	HOMO−1	18	33	32	17
	HOMO−2	7	17	29	47
	HOMO−3	7	21	29	33
	HOMO−4	2	4	35	59
	HOMO−5	3	5	22	69
4a	LUMO+2	56	40	4	0
	LUMO+1	53	32	15	0
	LUMO	31	11	34	24
	HOMO	14	56	18	12
	HOMO−1	2	20	4	74
	HOMO−2	5	20	8	67
	HOMO−3	19	18	46	17
	HOMO−4	4	8	7	81
6a	LUMO+1	22	19	20	39
	LUMO	27	14	30	29
	HOMO	19	22	53	6
	HOMO−1	23	21	51	5
	HOMO−2	2	22	3	73
	HOMO−3	3	25	3	69
	HOMO−4	23	2	62	13
	HOMO−5	2	2	5	91

[a]Contribution from each part of the molecule to the frontier orbitals (%).

participation of the $[Ag([24]aneS_8)]^+$ fragment is higher in the occupied orbitals HOMO, HOMO−1, and HOMO−4 and also in the case of the empty orbitals LUMO and LUMO+1 if we compare them with the corresponding frontier MOs for model **3a** (see Figure 8). In view of the contribution from each part of the molecule to the frontier orbitals we can anticipate that the participation of the silver(I)-crown thioether fragments is more important when the ligands bonded to the Au(I) centers are C_6F_5.

The first 10 singlet−singlet excitation energies were calculated for all model systems at the TD-DFT level of theory as described in the computational details. Since the lifetimes for complexes **2** and **3** lie in the microsecond range and they display larger Stokes shifts than complexes **4** and **6**, we also computed the lowest singlet−triplet excitation at TD-DFT level for the former (i.e., model systems **2a** and **3a**). We carried out the analysis of the excitation wavelengths, oscillator strengths, and orbitals involved in these electronic excitations, which can be related with the origin of the luminescent behavior observed experimentally. The results including the most important excitations are depicted in Table 8 and Figure 9.

The TD-DFT analysis of model $[Au(C_6Cl_5)_2Ag([14]aneS_4)]$ (**2a**) concludes that the most intense singlet−singlet excitations appear between 317 and 290 nm, whereas the lowest singlet−triplet excitation appears at 431 nm. These values agree well with the experimental excitation spectrum that displays a maximum at 273 nm and a low-energy shoulder at ca. 415 nm. The main contributions to the most intense theoretical electronic singlet−singlet excitation at 290 nm arise from the HOMO−2 → LUMO and HOMO−1 → LUMO transitions, respectively. In all three MOs the main contribution arises from the $[Au(C_6Cl_5)_2]^-$ unit with a smaller contribution from the $[Ag([12]aneS_4)]^+$ fragment. In view of these contributions we can assign this electronic excitation to internal transitions within the $[Au(C_6Cl_5)_2]^-$ units involving both the ligands and the metal, with a small contribution from a charge transfer from the aurate(I) fragment to the $[Ag([12]aneS_4)]^+$ one, due to the presence of the $Au^I\cdots Ag^I$ metallophilic interaction. The lowest singlet−triplet excitation computed theoretically also displays similar features. As can be observed in Table 8 the electronic excitation has three main contributions, in which the electron arises from HOMO−4, HOMO−2, and HOMO−1 and arrives to LUMO+2 or LUMO. The character of these orbitals leads to a similar assignment of the electronic transition, that is, as internal transitions within the $[Au(C_6Cl_5)_2]^-$ units involving both the ligands and the metal, with a contribution from a charge transfer from the aurate(I) fragment to the $[Ag([12]aneS_4)]^+$ one.

Model $[Au_2(C_6Cl_5)_4Ag_2([24]aneS_8)]$ (**3a**) also displays the most intense theoretical singlet−singlet excitations between 289 and 320 nm, whereas the lowest singlet−triplet calculated excitation appears at 434 nm. Again, these values are in agreement with the experimental excitation spectrum that shows a maximum at 277 nm and a low-energy shoulder at ca. 425 nm. The most intense singlet−singlet transition at 293 nm consists of the contribution of a HOMO−2 → LUMO and HOMO−3 → LUMO+1 transition. The character of the orbitals involved in these transitions is similar to the ones observed in model **2a**, that is, a main contribution from the orbitals of the $[Au(C_6Cl_5)_2]^-$ unit, although in this case the contribution from the $[Ag([24]aneS_8)]^+$ fragment to the occupied orbitals seems to be more important. In any case this electronic excitation can also be characterized as internal transitions within the $[Au(C_6Cl_5)_2]^-$ units involving both the ligands and the metal, with a contribution from a charge transfer from the aurate(I) to the $[Ag([24]aneS_8)]^+$ fragment. Similarly, the singlet−triplet electronic excitation involves the contribution of the same MOs, except HOMO−3, as the previous singlet−singlet excitation, which leads to a similar assignment of this forbidden transition.

The TD-DFT analysis of the most important singlet−singlet transition computed for model $[Au_2(C_6F_5)_4Ag_2([9]aneS_3)_4]$ (**4a**) shows a very strong excitation at 325 nm (experimental value 340 nm) between HOMO and LUMO orbitals. The character of these orbitals is now shared between the Au^I and Ag^I fragments, this being the most important difference between this model and the previous ones bearing C_6Cl_5 ligands, mostly located on the aurate(I) units. In this case the assignment of the singlet−singlet excitation for model **4a** is similar to that for models **2a** and **3a**, although with a larger contribution from the $[Ag([9]aneS_3)_2]^+$ fragments.

The last model analyzed through TD-DFT calculations, $[Au_2(C_6F_5)_4Ag_2([24]aneS_8)]$ (**6a**), displays two strong singlet−singlet transitions at 294 and 279 nm (Table 8). The experimental excitation spectrum ranges from 250 to 400 nm with decreasing intensity. The analysis of these two theoretical

dx.doi.org/10.1021/ic501515c | Inorg. Chem. 2014, 53, 10471−10484

Table 8. TD-DFT First Singlet−Singlet Excitation Calculations for Model Systems 2a, 3a, 4a, and 6a and Lowest Singlet−Triplet Excitations for Models 2a and 3a

model	exc.[a]	λ_{calc} (nm)	f (s)[b]	contributions[c]	origin
2a	$S_0 \rightarrow S_1$	317.4	0.0229	HOMO→ LUMO (95.2)	
	$S_0 \rightarrow S_2$	308.7	0.0639	HOMO−2→ LUMO (16.4)	
				HOMO−1→ LUMO (76.4)	
	$S_0 \rightarrow S_3$	289.9	0.3034	HOMO−2→ LUMO (75.3)	
				HOMO−1→ LUMO (18.1)	
	$S_0 \rightarrow T_1$	430.7		HOMO−4→ LUMO+2 (17.2)	$\pi-\pi^*$
				HOMO−2→ LUMO (15.2)	Au−π^*
				HOMO−1→ LUMO (17.8)	(ML)(M′L′)CT
3a	$S_0 \rightarrow S_1$	320.2	0.1486	HOMO−1→ LUMO+1 (41.2)	
				HOMO→ LUMO (49.9)	
	$S_0 \rightarrow S_4$	293.4	0.2986	HOMO−3→ LUMO+1 (35.1)	
				HOMO−2→ LUMO (42.1)	
	$S_0 \rightarrow S_8$	288.9	0.0683	HOMO−5→ LUMO+1 (22.4)	
				HOMO−4→ LUMO (15.3)	
				HOMO−1→ LUMO+1 (22.3)	
				HOMO→ LUMO (23.7)	
	$S_0 \rightarrow T_1$	434.0		HOMO→ LUMO (53.3)	Au−π^*
4a	$S_0 \rightarrow S_1$	324.6	0.7360	HOMO→ LUMO (96.7)	(ML)(M′L′)CT
					Au−π^*
	$S_0 \rightarrow S_3$	291.3	0.0143	HOMO→ LUMO+1 (73.2)	
	$S_0 \rightarrow S_4$	280.7	0.1805	HOMO−2→ LUMO (95.0)	
	$S_0 \rightarrow S_7$	273.9	0.0286	HOMO−3→ LUMO (61.7)	
				HOMO→ LUMO+2 (9.9)	
	$S_0 \rightarrow S_8$	272.1	0.0263	HOMO−4→ LUMO (79.4)	
6a	$S_0 \rightarrow S_1$	294.0	0.3239	HOMO−1→ LUMO (59.9)	(ML)(M′L′)CT
				HOMO→ LUMO+1 (35.9)	
	$S_0 \rightarrow S_4$	278.8	0.5105	HOMO−3→ LUMO+1 (29.9)	(ML)(M′L′)CT
				HOMO−2→ LUMO (52.7)	
	$S_0 \rightarrow S_5$	271.1	0.0299	HOMO−1→ LUMO (27.5)	
				HOMO→ LUMO+1 (47.4)	
	$S_0 \rightarrow S_{10}$	257.5	0.0199	HOMO−5→ LUMO (34.1)	
				HOMO−4→ LUMO+1 (40.7)	

[a]Only excitations with larger oscillator strengths are included among the first 10 singlet excitation calculations. [b]Oscillator strength (f) shows the mixed representation of both velocity and length representations. [c]Value is 2 × |coeff|^2 ×100

excitations also points to a higher contribution from the $[Ag([24]aneS_8)]^+$ fragments to the orbitals involved in the electronic transitions (HOMO, HOMO-1, HOMO-2, HOMO−3, LUMO, and LUMO+1). Therefore, the assignment of the electronic excitations can be ascribed to internal transitions within the $[Au(C_6F_5)_2]^-$ units involving both the ligands and the metal, together with a contribution from a charge transfer from the aurate(I) to the $[Ag([24]aneS_8)]^+$ fragment observed in the contributions from HOMO−1 and HOMO−3 to LUMO and LUMO+1.

In conclusion, although several parameters can affect the emissive properties of these heterometallic Au^I/Ag^I complexes, it seems that the change in the perhalophenyl ligands bonded to the Au^I center in the aurate(I) units lead to a lower (C_6Cl_5) or higher (C_6F_5) participation of the silver(I)-crown thioether fragments in the electronic transitions related to the emissive properties of the complexes studied. These fragments constitute the most flexible parts of the molecules, and probably the transitions with higher participation of the silver(I)-crown thioether cationic fragments favor a more effective nonradiative deactivation pathway, reducing the efficiency of the emissions, as observed experimentally. Therefore, a careful choice of the perhalophenyl groups can lead to a higher or lower contribution of the silver(I)-crown thioether parts and to the intensity of the emissions.

CONCLUSIONS

Heteronuclear complexes $[\{Au(C_6X_5)_2\}Ag(L)_x]$ formed via Ag−S bonds and Au···Ag contacts are obtained by treatment of $[\{Au(C_6X_5)_2\}Ag]_n$ (X = Cl, F) with the crown thioethers 1,4,7-trithiacyclononane ([9]aneS$_3$), 1,4,8,11-tetrathiacyclotetradecane ([14]aneS$_4$), or 1,4,7,10,13,16,19,22-octathiacyclotetracosane ([24]aneS$_8$). X-ray diffraction studies reveal that the nature of the macrocyclic ligand rules both the number of ligands bonded to silver (L = [9]aneS$_3$, x = 2 (**1**, **4**); L = [14]aneS$_4$, x = 1 (**2**, **5**); L = [24]aneS$_8$, x = 0.5 (**3**, **6**)) and the presence of aurophilic interactions. It is noteworthy that complex **2** represents the first example of a dinuclear Au/Ag compound displaying an unsupported Au···Ag contact. Moreover, the pentachlorophenyl complexes show Ag···C_{ipso} contacts, which are not present in the pentafluorophenyl compounds, as well as shorter Au···Ag distances, with a simultaneous increasing of the strength of both types of interactions.

Regardless of the presence of aurophilic interactions, all the complexes are luminescent in the solid state, showing that such contacts are not needed to display luminescence. Neither the

dx.doi.org/10.1021/ic501515c | Inorg. Chem. 2014, 53, 10471−10484

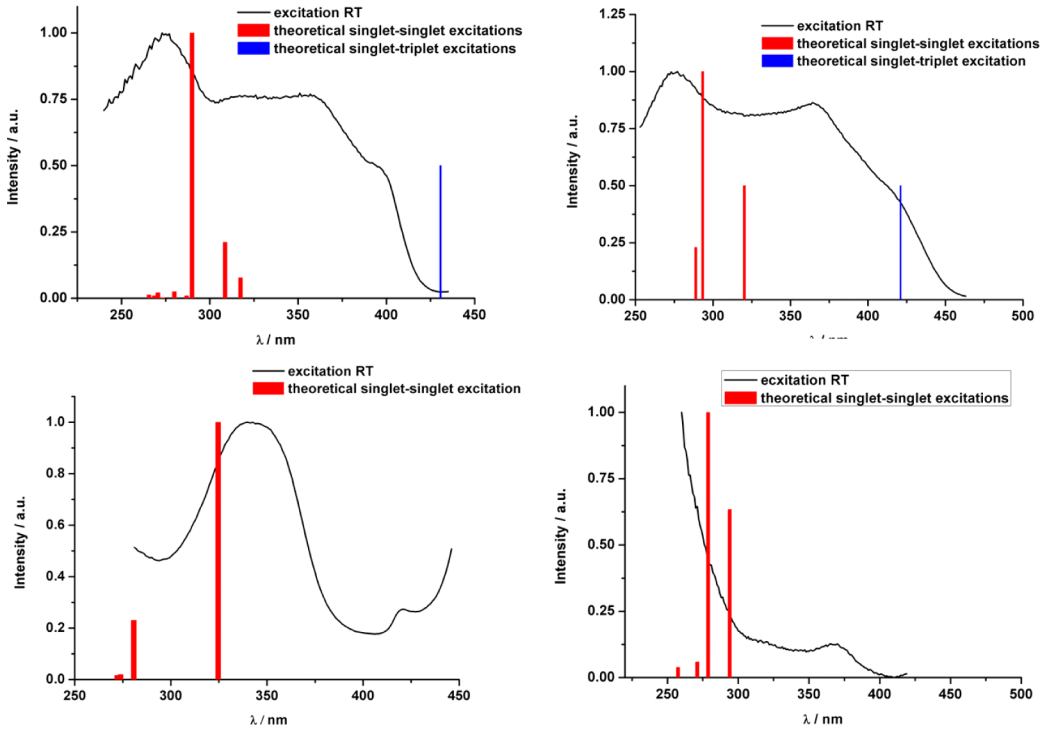

Figure 9. Experimental excitation spectra and TD-DFT first singlet−singlet (red) excitation calculations for model systems **2a** (upper-left), **3a** (upper-right), **4a** (lower-left), and **6a** (lower-right). The lowest singlet−triplet (blue) excitations for models **2a** and **3a** are also included. The blue bars only represent the energy of the lowest-singlet−triplet transitions since the oscillator strength cannot be estimated.

strength of the Au···Ag interactions nor the structural disposition determine the efficiency of the luminescence of the complexes. Although a direct relationship between the number or nature of ligands in the complexes and their optical properties is not observed, in general the perchlorophenyl derivatives are strongly luminescent, while the fluorinated complexes display weak luminescence. Thus, the perhalophenyl ligand bonded to gold(I) seems to be the key factor, also in accord with the DFT and TD-DFT calculations, which points to a lower participation of the silver(I)-crown thioether moieties in the lowest empty MOs of the highly emissive compounds, which, as in the experimental measurements, correspond to the C_6Cl_5 containing derivatives. Thus, in the case of the C_6Cl_5-containing complex **2** the most important contributions to the singlet−triplet transitions related to the emissive behavior are of $\pi \rightarrow \pi^*$ and Au $\rightarrow \pi^*$ origin with some charge transfer contribution from the aurate(I) unit (ML) to the Ag-thioether moiety (MLM′L′CT). In the case of the C_6Cl_5-containing complex **3** the origin of the emissive behavior is an internal singlet−triplet Au $\rightarrow \pi^*$ transition. In contrast, the C_6F_5-complex **4** displays a strong singlet−singlet transition that consists of a charge transfer contribution from the aurate(I) unit (ML) to the Ag-thioether moiety (M′L′) (MLM′L′CT) with a minor contribution from an internal Au $\rightarrow \pi^*$ transition. Finally, the C_6F_5-containing complex **6** displays two strong singlet−singlet transitions, which are both related to the above-mentioned charge transfer contribution from the aurate(I) unit (ML) to the Ag-thioether moiety (M′L′) (MLM′L′CT). The weakest singlet−singlet transitions also contribute to the absoprtion spectrum, although with different origins.

EXPERIMENTAL SECTION

General. Thioether crown ligands $[\{Au(C_6Cl_5)_2\}Ag]_n$ and $[\{Au(C_6F_5)_2\}Ag]_n$ were prepared according to the literature.[25]

Instrumentation. Fourier transform infrared (FT-IR) spectra were recorded in the 4000−200 cm^{-1} range on a Nicolet Nexus FT-IR spectrometer using Nujol mulls between polyethylene sheets. C, H, and S analyses were carried out with PerkinElmer 240C microanalyzer. Molar conductivities were measured in ca. 5×10^{-4} M acetone solutions with a Jenway 4510 conductimeter. Mass spectra were recorded with a Bruker Microflex matrix-assisted laser desorption ionization time-of-flight mass spectrometer (MALDI-TOF MS) using dithranol (DIT) or 11-dicyano-4-*tert*-butylphenyl-3-methylbutadiene (DCTB) as matrix. ^1H and ^{19}F NMR spectra were recorded with a Bruker Avance 400 spectrometer in $[D_8]$-THF (**1** and **4**−**6**) or in $[D_6]$-dimethyl sulfoxide (**2** and **3**). Chemical shifts are quoted relative to $SiMe_4$ (^1H, external) and $CFCl_3$ (^{19}F, external). Excitation and emission spectra in the solid state were recorded with a Jobin−Yvon Horiba Fluorolog 3−22 Tau-3 spectrofluorimeter. Lifetime measurements were recorded with a Datastation HUB-B with a nanoLED controller and DAS6 software. The nanoLED employed for lifetime measurements was one of 370 nm with pulse lengths of 0.8−1.4 ns. The lifetime data were fitted with the Jobin−Yvon software package. Luminescence quantum yields in the solid state were measured with an integrating sphere accessory. Measurements at 77 K were done with an Oxford Cryostat Optistat DN with an accessory for solid samples.

*Synthesis. [{Au(C$_6$Cl$_5$)$_2$}Ag([9]aneS$_3$)$_2$] (**1**).* To a well-stirred solution of $[\{Au(C_6Cl_5)_2\}Ag]_n$ (50 mg, 0.062 mmol) in THF (20 mL), [9]aneS$_3$ (22 mg, 0.124 mmol) was added. The mixture was stirred at room temperature for 3 h, after which the solvent was partially removed under reduced pressure. The addition of *n*-hexane led to the precipitation of complex **1** as a yellow solid that was filtered off and washed with *n*-hexane. Yield 60.2 mg, 83% (based on the metallic precursor). Elemental analysis (%) calcd for $C_{48}H_{48}Ag_2Au_2Cl_{20}S_{12}$ (MW 2328.41): C 24.76, H 2.08, S 16.53. Found: C 25.17, H 2.20, S 16.26. Λ_M: 97 Ω^{-1} cm^2 mol^{-1}. ^1H NMR (400 MHz, $[D_8]$-THF, ppm): δ 2.92 (s, 12 H, CH_2). MALDI-TOF(−) *m*/*z* (%): 695 $[Au(C_6Cl_5)_2]^-$ (100). MALDI-TOF(+) *m*/*z*

dx.doi.org/10.1021/ic501515c | *Inorg. Chem.* 2014, 53, 10471−10484

(%): 469 [Ag([9]aneS$_3$)$_2$]$^+$ (100). FT-IR (Nujol): ν([Au(C$_6$Cl$_5$)$_2$]$^-$) at 834 and 614 cm^{-1}.

[{Au(C$_6$Cl$_5$)$_2$}Ag([14]aneS$_4$)] (2). [14]aneS$_4$ (33 mg, 0.124 mmol) was added to a solution of [{Au(C$_6$Cl$_5$)$_2$}Ag]$_n$ (100 mg, 0.124 mmol) in tetrahydrofuran (20 mL). After 3 h of stirring, the solution was concentrated under vacuum. Addition of *n*-hexane led to the precipitation of product **2** as a white solid that was filtered off and washed with *n*-hexane. Yield 111.9 mg, 84% (based on the metallic precursor). Elemental analysis (%) calcd for C$_{44}$H$_{40}$Ag$_2$Au$_2$Cl$_{20}$S$_8$ (MW 2144.04): C 24.65, H 1.88, S 11.96. Found: C 24.63, H 1.97, S 11.95. ^{1}H NMR (400 MHz, [D$_6$]-dimethyl sulfoxide, ppm): δ 1.86 (q, 4H, S−CH$_2$−C*H*$_2$−CH$_2$−S, $^3J_{(H-H)}$ = 2 Hz), 2.68 (t, 8H, S−C*H*$_2$−CH$_2$−C*H*$_2$−S, $^3J_{(H-H)}$ = 2 Hz), 2.79 (s, 8H, S−C*H*$_2$−C*H*$_2$−S). MALDI-TOF(−) *m*/*z* (%): 695 [Au(C$_6$Cl$_5$)$_2$]$^-$ (100). MALDI-TOF(+) *m*/*z* (%): 377 [Ag([14]aneS$_4$)]$^+$ (100). FT-IR (Nujol): ν([Au(C$_6$Cl$_5$)$_2$]$^-$) at 834 and 614 cm^{-1}.

[{Au(C$_6$Cl$_5$)$_2$}$_2$Ag$_2$([24]aneS$_8$)] (3). [24]aneS$_8$ (30 mg, 0.062 mmol) was added to a solution of [{Au(C$_6$Cl$_5$)$_2$}Ag]$_n$ (100 mg, 0.124 mmol) in tetrahydrofuran (20 mL). After 3 h of stirring, the solution was concentrated under vacuum. Addition of *n*-hexane led to the precipitation of product **3** as a white solid that was filtered and washed with *n*-hexane. Yield 89.8 mg, 69% (based on the metallic precursor). Elemental analysis (%) calcd for C$_{40}$H$_{32}$Ag$_2$Au$_2$Cl$_{20}$S$_8$ (2087.93): C 23.01, H 1.54, S 12.29. Found: C 23.23, H 1.77, S 12.75. ^{1}H NMR (400 MHz, [D$_6$]-dimethyl sulfoxide, ppm): δ 2.90 (s, 32 H, C*H*$_2$). MALDI-TOF(−) *m*/*z* (%): 695 [Au(C$_6$Cl$_5$)$_2$]$^-$ (100). MALDI-TOF(+) *m*/*z* (%): 589 [Ag([24]aneS$_8$)]$^+$ (100). FT-IR (Nujol): ν([Au(C$_6$Cl$_5$)$_2$]$^-$) at 834 and 614 cm^{-1}.

[{Au(C$_6$F$_5$)$_2$}Ag([9]aneS$_3$)$_2$]$_2$ (4). To a well-stirred solution of [{Au(C$_6$F$_5$)$_2$}Ag]$_n$ (50 mg, 0.078 mmol) in toluene (20 mL) [9]aneS$_3$ (28 mg, 0.157 mmol) was added. The mixture was stirred at room temperature for 3 h, then the solvent was partially removed under reduced pressure and finally, the addition of *n*-hexane led to the precipitation of product **4** as a white solid that was filtered and washed with *n*-hexane. Yield 67.2 mg, 86% (based on the metallic precursor). Elemental analysis (%) calcd for C$_{48}$H$_{48}$Ag$_2$Au$_2$F$_{20}$S$_{12}$ (MW 1999.32): C 29.18, H 2.82, S 19.80. Found: C 29.25, H 2.86, S 19.85. Λ_M: 66 Ω^{-1}cm^2 mol^{-1}. ^{1}H NMR (400 MHz, [D$_8$]tetrahydrofuran, ppm): δ 3.01 (*s*, 12 H, C*H*$_2$). ^{19}F NMR (376 MHz, [D$_8$]-THF, ppm): δ −110.8 (m, 2F, F$_o$), −158.1 (t, 1F, F$_p$, $^3J_{(Fp-Fm)}$ = 19.8 Hz), −161.3 (m, 2F, F$_m$). MALDI-TOF(−) *m*/*z* (%): 531 [Au(C$_6$F$_5$)$_2$]$^-$ (100). MALDI-TOF(+) *m*/*z* (%): 287 [Ag([9]aneS$_3$)]$^+$ (22), 469 [Ag([9]aneS$_3$)$_2$]$^+$ (100), 1107 [Au(C$_6$F$_5$)$_2$Ag$_2$([9]aneS$_3$)$_2$] (12). FT-IR (Nujol): ν([Au(C$_6$F$_5$)$_2$]$^-$) at 1506, 953, and 787 cm^{-1}.

[{Au(C$_6$F$_5$)$_2$}Ag([14]aneS$_4$)]$_2$ (5). [14]aneS$_4$ (42 mg, 0.156 mmol) was added to a solution of [{Au(C$_6$F$_5$)$_2$}Ag]$_n$ (100 mg, 0.156 mmol) in toluene (20 mL). After 3 h of stirring, the solution was concentrated under vacuum, leading to the precipitation of product **5** as a white solid that was filtered off and washed with *n*-hexane. Yield 92.3 mg, 65% (based on the metallic precursor). Elemental analysis (%) calcd for C$_{44}$H$_{40}$Ag$_2$Au$_2$F$_{20}$S$_8$ (MW 1814.96): C 29.14, H 2.23, S 14.12. Found: C 29.06, H 2.18, S 14.08. Λ_M: 90 Ω^{-1}cm^2 mol^{-1}. ^{1}H NMR (400 MHz, [D$_8$]-THF, ppm): δ 2.03 (*q*, 4H, S−CH$_2$−C*H*$_2$−CH$_2$−S, $^3J_{(H-H)}$ = 2 Hz), 2.85 (t, 8H, S−C*H*$_2$−CH$_2$−C*H*$_2$−S, $^3J_{(H-H)}$ = 2 Hz), 2.87 (s, 8H, S−C*H*$_2$−C*H*$_2$−S). ^{19}F NMR (376 MHz, [D$_8$]-THF, ppm): δ −110.8 (m, 2F, F$_o$), −158.7 (t, 1F, F$_p$, $^3J_{(Fp-Fm)}$ = 19.8 Hz), −161.4 (m, 2F, F$_m$). MALDI-TOF(−) *m*/*z* (%): 531 [Au(C$_6$F$_5$)$_2$]$^-$ (100). MALDI-TOF(+) *m*/*z* (%): 377 [Ag([14]aneS$_4$)]$^+$ (100). FT-IR (Nujol): ν([Au(C$_6$F$_5$)$_2$]$^-$) at 1505, 952, and 787 cm^{-1}.

[{Au(C$_6$F$_5$)$_2$}$_2$Ag$_2$([24]aneS$_8$)] (6). [24]aneS$_8$ (38 mg, 0.078 mmol) was added to a solution of [{Au(C$_6$F$_5$)$_2$}Ag]$_n$ (100 mg, 0.156 mmol) in toluene (20 mL). After 3 h of stirring, the solution was concentrated under vacuum, led to the precipitation of product **6** as a white solid that was filtered and washed with *n*-hexane. Yield 124.3 mg, 90% (based on the metallic precursor). Elemental analysis (%) calcd for C$_{40}$H$_{32}$Ag$_2$Au$_2$F$_{20}$S$_8$ (MW 1758.85): C 27.31, H 1.83, S 14.58. Found: C 27.36, H 1.78, S 14.54. Λ_M: 159 Ω^{-1}cm^2 mol^{-1}. ^{1}H NMR (400 MHz, [D$_8$]tetrahydrofuran, ppm): δ 3.08 (*s*, 32 H, C*H*$_2$). ^{19}F NMR (376 MHz, [D$_8$]-THF, ppm): δ −111.3 (m, 2F, F$_o$), −159.8 (t, 1F, F$_p$, $^3J_{(Fp-Fm)}$ = 19.8 Hz), −161.4 (m, 2F, F$_m$). MALDI-TOF(−) *m*/*z* (%): 531 [Au(C$_6$F$_5$)$_2$]$^-$ (100). MALDI-TOF(+) *m*/*z* (%): 589 [Ag([24]-aneS$_8$)]$^+$ (100), 1227 [Au(C$_6$F$_5$)$_2$Ag$_2$([24]aneS$_8$)]$^+$ (18). FT-IR (Nujol): ν([Au(C$_6$F$_5$)$_2$]$^-$) at 1502, 958, and 781 cm^{-1}.

Crystallography. Crystals were mounted in inert oil on glass fibers and transferred to a Bruker SMART APEX diffractometer (for **2**) or a Nonius Kappa CCD diffractometer (for **3**, **4**, and **6**), both equipped with an Oxford Cryosystems open-flow cryostat. Data were collected as ω and ϕ scans using monochromated Mo Kα radiation (λ = 0.710 73 Å). Absorption effects were treated by semiempirical corrections based on multiple scans. The structures were solved by direct methods and refined on F^2 using the program SHELXL-97.[36] All non-hydrogen atoms were refined anisotropically, and hydrogen atoms were included using riding model. Further details of the data collection and refinement are given in Table 1. Selected bond lengths and angles are collected in Tables 2−5 and crystal structures of complexes **2**, **3**, **4**, and **6** are shown in Figures 1 and 2. Supplementary crystallographic data are also available in the Supporting Information.

Computational Details. All calculations were carried out using the Gaussian 09 package.[37] DFT and TD-DFT calculations were carried out using the PBE functional.[38] The following basis set combinations were employed for the metals Au and Ag: the 19-VE pseudopotentials from Stuttgart and the corresponding basis sets augmented with two f polarization functions[39] were used for the metals Au and Ag. The heteroatoms were treated by Stuttgart pseudopotentials,[40] including only the valence electrons for each atom. For these atoms double-ζ basis sets of ref 38 were used, augmented by d-type polarization functions.[41] For the H atom, a double-ζ and a p-type polarization function was used.[42] All the calculations were performed on model systems for complexes **2**−**4** and **6** built up from their corresponding X-ray structures. Overlap populations between molecular fragments were calculated using the AOMix program[43,44] with C^2 population analysis (SCPA) option.[45]

■ ASSOCIATED CONTENT

Ⓢ Supporting Information

X-ray crystallographic data for complexes **2**−**4** and **6** in CIF format. This material is available free of charge via the Internet at http://pubs.acs.org. CCDC-1009315−1009318 contains the supplementary crystallographic data for this paper. These data can be obtained free of charge via www.ccdc.cam.ac.uk/conts/retrieving.html (or from the Cambridge Crystallographic Data Centre, 12 Union Road, Cambridge CB2 1EZ, UK; fax: (+44) 1223−336−033; or e-mail: deposit@ccdc.cam.ac.uk).

■ AUTHOR INFORMATION

Corresponding Authors

*E-mail: lippolis@unica.it. (V.L.)
*E-mail: josemaria.lopez@unirioja.es. (J.M.L.)
*E-mail: m-elena.olmos@unirioja.es. (M.E.O.)

Notes

The authors declare no competing financial interest.

■ ACKNOWLEDGMENTS

D.G.I. (MEC)/FEDER (Project No. CTQ2013−48635-C2-2P) and MIUR (Project No. PRIN 2009−2009Z9ASCA) are acknowledged for financial support.

■ REFERENCES

(1) (a) Pyykkö, P.; Zhao, Y.-F. *Angew. Chem., Int. Ed. Engl.* **1991**, *30*, 604. (b) Pyykkö, P.; Li, J.; Runeberg, N. *Chem. Phys. Lett.* **1994**, *218*, 133.

(2) (a) Schmidbaur, H. Gold-Progress in Chemistry. In *Biochemistry and Technology;* John Wiley & Sons, Inc.: New York, 1999. (b) Schmidbaur, H. *Nature* **2001**, *413*, 31. (c) Schmidbaur, H. *Gold Bull.* **1990**, *23*, 11.

(3) See, for example: (a) Chan, C. K.; Guo, C. X.; Cheng, K. K.; Li, D.; Che, C. M. *J. Chem. Soc., Dalton Trans.* **1994**, 3677. (b) Fernández, E. J.; López-de-Luzuriaga, J. M.; Monge, M.; Rodríguez, M. A.; Crespo, O.; Gimeno, M. C.; Laguna, A.; Jones, P. G. *Chem.—Eur. J.* **2000**, *6*, 636. and references therein (c) Burini, A.; Braver, R.; Fackler, J. P., Jr.; Galassi, R.; Grant, T. A.; Omary, M. A.; Pietroni, B. R.; Staples, R. J. *Inorg. Chem.* **2000**, *39*, 3158. (d) Fernández, E. J.; Gimeno, M. C.; Laguna, A.; López-de-Luzuriaga, J. M.; Monge, M.; Pyykkö, P.; Sundholm, D. *J. Am. Chem. Soc.* **2000**, *122*, 7287.

(4) (a) Wang, S.; Fackler, J. P., Jr.; King, C.; Wang, J. C. *J. Am. Chem. Soc.* **1988**, *110*, 3308. (b) Wang, S.; Garzón, G.; King, C.; Wang, J. C.; Fackler, J. P., Jr. *Inorg. Chem.* **1989**, *28*, 4623. (c) Crespo, O.; Fernández, E. J.; Jones, P. G.; Laguna, A.; López-de-Luzuriaga, J. M.; Mendía, A.; Monge, M.; Olmos, M. E. *Chem. Commun.* **1998**, 2233. (d) Catalano, V. J.; Bennett, B. L.; Kar, H. M.; Noll, B. C. *J. Am. Chem. Soc.* **1999**, *121*, 10235.

(5) (a) Burini, A.; Fackler, J. P., Jr.; Galassi, R.; Grant, T. A.; Omary, M. A.; Rawashded-Omary, M. A.; Pietroni, B. R.; Staples, R. J. *J. Am. Chem. Soc.* **2000**, *122*, 11264. (b) López-de-Luzuriaga, J. M.; Monge, M.; Olmos, M. E.; Pascual, D. *Inorg. Chem.* **2014**, *53*, 1275.

(6) Fernández, E. J.; Laguna, A.; López-de-Luzuriaga, J. M.; Monge, M.; Nema, M.; Olmos, M. E.; Pérez, J.; Silvestru, C. *Chem. Commun.* **2007**, 571.

(7) Bojan, R. V.; López-de-Luzuriaga, J. M.; Monge, M.; Olmos, M. E.; Echeverría, R.; Lehtonen, O.; Sundholm, D. *ChemPlusChem* **2014**, *79*, 67.

(8) Bauer, A.; Schmidbaur, H. *J. Am. Chem. Soc.* **1996**, *118*, 5450.

(9) (a) Chen, J. X.; Zhang, W. H.; Tang, X. Y.; Ren, Z. G.; Li, H. X.; Zhang, Y.; Lang, J. P. *Inorg. Chem.* **2006**, *45*, 7671. (b) Fernández, E. J.; Laguna, A.; López-de-Luzuriaga, J. M.; Monge, M.; Montiel, M.; Olmos, M. E.; Pérez, J.; Puelles, R. C.; Sáenz, J. C. *Dalton Trans.* **2005**, 1162. (c) Fernández, E. J.; Laguna, A.; López-de-Luzuriaga, J. M.; Monge, M.; Montiel, M.; Olmos, M. E.; Rodríguez-Castillo, M. *Dalton Trans.* **2009**, 7509. (d) Fernández, E. J.; López-de-Luzuriaga, J. M.; Monge, M.; Olmos, M. E.; Pérez, J.; Laguna, A. *J. Am. Chem. Soc.* **2002**, *124*, 5942. (e) Fernández, E. J.; Laguna, A.; López-de-Luzuriaga, J. M.; Olmos, M. E.; Pérez, J. *Chem. Commun.* **2003**, 1760. (f) Fernández, E. J.; Laguna, A.; López-de-Luzuriaga, J. M.; Monge, M.; Montiel, M.; Olmos, M. E. *Inorg. Chem.* **2007**, *46*, 2953.

(10) (a) Fernández, E. J.; Laguna, A.; Lasanta, T.; López-de-Luzuriaga, J. M.; Montiel, M.; Olmos, M. E. *Organometallics* **2008**, *27*, 2971. (b) Fernández, E. J.; Laguna, A.; López-de-Luzuriaga, J. M.; Monge, M.; Montiel, M.; Olmos, M. E.; Rodríguez-Castillo, M. *Organometallics* **2006**, *25*, 3639. (c) López-de-Luzuriaga, J. M.; Monge, M.; Olmos, M. E.; Pascual, P.; Lasanta, T. *Chem. Commun.* **2011**, 6795. (d) Fernández, E. J.; Jones, P. G.; Laguna, A.; López-de-Luzuriaga, J. M.; Monge, M.; Olmos, M. E.; Puelles, R. C. *Organometallics* **2007**, *26*, 5931. (e) Laguna, A.; Lasanta, T.; López-de-Luzuriaga, J. M.; Monge, M.; Naumov, P.; Olmos, M. E. *J. Am. Chem. Soc.* **2010**, *132*, 456.

(11) (a) Fernández, E. J.; Jones, P. G.; Laguna, A.; López-de-Luzuriaga, J. M.; Monge, M.; Pérez, J.; Olmos, M. E. *Inorg. Chem.* **2002**, *41*, 1056. (b) Fernández, E. J.; Laguna, A.; López-de-Luzuriaga, J. M.; Olmos, M. E.; Pérez, J. *Dalton Trans.* **2004**, 1801. (c) Fernández, E. J.; Laguna, A.; López-de-Luzuriaga, J. M.; Montiel, M.; Olmos, M. E.; Pérez, J.; Puelles, R. C. *Organometallics* **2006**, *25*, 4307.

(12) See, for example: (a) Fernández, E. J.; Garau, A.; Laguna, A.; Lasanta, T.; Lippolis, V.; López-de-Luzuriaga, J. M.; Montiel, M.; Olmos, M. E. *Organometallics* **2010**, *29*, 2951. (b) Fernández, E. J.; Laguna, A.; Lasanta, T.; López-de-Luzuriaga, J. M.; Montiel, M.; Olmos, M. E. *Inorg. Chim. Acta* **2010**, *363*, 1965.

(13) (a) Fernández, E. J.; Jones, P. G.; Laguna, A.; López-de-Luzuriaga, J. M.; Monge, M.; Montiel, M.; Olmos, M. E.; Pérez, J. *Z. Naturforsch.* **2004**, *59b*, 1379. (b) Fernández, E. J.; Laguna, A.; López-de-Luzuriaga, J. M.; Montiel, M.; Olmos, M. E.; Pérez, J. *Organometallics* **2005**, *24*, 1631.

(14) Fernández, E. J.; López-de-Luzuriaga, J. M.; Monge, M.; Olmos, M. E.; Puelles, R. C.; Laguna, A.; Mohamed, A. A.; Fackler, J. P., Jr. *Inorg. Chem.* **2008**, *47*, 8069.

(15) Fernández, E. J.; Laguna, A.; López-de-Luzuriaga, J. M.; Monge, M.; Montiel, M.; Olmos, M. E. *Inorg. Chem.* **2005**, *44*, 1163.

(16) (a) Fernández, E. J.; Laguna, A.; López-de-Luzuriaga, J. M.; Mendizábal, F.; Monge, M.; Olmos, M. E.; Pérez, J. *Chem.—Eur. J.* **2003**, *9*, 456. (b) Fernández, E. J.; López-de-Luzuriaga, J. M.; Monge, M.; Olmos, M. E.; Pérez, J.; Laguna, A.; Mohamed, A. A.; Fackler, J. P., Jr. *J. Am. Chem. Soc.* **2003**, *125*, 2022. (c) Fernández, E. J.; Laguna, A.; López-de-Luzuriaga, J. M.; Olmos, M. E.; Pérez, J. *Organometallics* **2006**, *25*, 1689. (d) Fernández, E. J.; Laguna, A.; López-de-Luzuriaga, J. M.; Monge, M.; Mendizábal, F. *J. Mol. Struct.* **2008**, *851*, 121.

(17) (a) Usón, R.; Laguna, A.; Laguna, M.; Jones, P. G.; Sheldrick, G. M. *Chem. Commun.* **1981**, 1097. (b) Usón, R.; Laguna, A.; Laguna, M.; Manzano, B. R.; Jones, P. G.; Sheldrick, G. M. *J. Chem. Soc., Dalton Trans.* **1984**, 285.

(18) See, for example: (a) Cooper, S. R.; Rawle, S. C. *Bioinorganic Chemistry;* Springer-Verlag: Berlin, Heidelberg, 1990; Vol *72*. (b) Cooper, S. R. *Acc. Chem. Res.* **1988**, *21*, 141. (c) Blake, A. J.; Schröder, M. *Adv. Inorg. Chem.* **1990**, *35*, 1. (d) Adachi, T.; Durrant, M. D.; Hughes, D. L.; Pickett, C. J.; Richards, R. L.; Talarmin, J.; Yoshiba, T. *J. Chem. Soc., Chem. Commun.* **1992**, 1464. (e) Landgrafe, C.; Sheldrick, W. S. *J. Chem. Soc., Dalton. Trans.* **1996**, 989. (f) Adams, R. D.; Fallon, S. B.; Perrin, J. L.; Queisser, J. A.; Yamamoto, J. H. *Chem. Ber.* **1996**, *129*, 313. (g) Kim, H.-J.; Lee, J.-H.; Suh, I.-H.; Do, Y. *Inorg. Chem.* **1995**, *34*, 796.

(19) Shaw, J. L.; Wolowska, J.; Collison, D.; Howard, J. A. K.; McInnes, E. J. L.; McMaster, J.; Blake, A. J.; Wilson, C.; Schröder, M. *J. Am. Chem. Soc.* **2006**, *128*, 13827.

(20) (a) Robinson, G. H.; Zhang, H.; Atwood, J. L. *Organometallics* **1987**, *6*, 887. (b) George, K.; Jura, M.; Levason, W.; Light, M. E.; Ollivere, L. P.; Reid, G. *Inorg. Chem.* **2012**, *51*, 2231. (c) Gurnani, C.; Jura, M.; Levason, W.; Ratnani, R.; Reid, G.; Webster, M. *Dalton Trans.* **2009**, 1611. (d) Blake, A. J.; Fenske, D.; Li, W.-S.; Lippolis, V.; Schröder, M. *J. Chem. Soc., Dalton Trans.* **1998**, 3961. (e) Blake, A. J.; Greig, J. A.; Schröder, M. *J. Chem. Soc., Dalton Trans.* **1991**, 529. (f) Cheng, F.; Hector, A. L.; Levason, W.; Reid, G.; Webster, M.; Zhang, W. *Chem. Commun.* **2008**, 5508. (g) Willey, G. R.; Jarvis, A.; Palin, J.; Errington, W. *J. Chem. Soc., Dalton Trans.* **1994**, 255. (h) Kuppers, H.-J.; Wieghardt, K.; Nuber, B.; Weiss, J. *Z. Anorg. Allg. Chem.* **1989**, *577*, 155. (i) Willey, G. R.; Lakin, M. T.; Ravindra, M.; Alcock, N. W. *Chem. Commun.* **1991**, 271.

(21) (a) Sanaullah; Kano, K.; Glass, R. S.; Wilson, G. S. *J. Am. Chem. Soc.* **1993**, *115*, 592. (b) Wyer, E.; Giuccardo, G.; Leigh, V.; Muller-Bunz, H.; Albrecht, M. *J. Organomet. Chem.* **2011**, *696*, 2882. (c) Blake, A. J.; Champness, N. R.; Howdle, S. M.; Webb, P. E. *Inorg. Chem.* **2000**, *39*, 1035. (d) Parker, D.; Roy, P. S.; Ferguson, G.; Hunt, M. M. *Inorg. Chim. Acta* **1989**, *155*, 227. (e) Setzer, W. N.; Guo, Q.; Grant, G. J.; Hubbard, J. L.; Glass, R. S.; VanDerveer, D. G. *Heteroat. Chem.* **1990**, *1*, 317. (f) Helm, M. L.; Hill, L. L.; Lee, J. P.; VanDerveer, D. G.; Grant, G. J. *Dalton Trans.* **2006**, 3534. (g) Wilhelm, M.; Deeken, S.; Berssen, E.; Saak, W.; Lutzen, A.; Koch, R.; Strasdeit, H. *Eur. J. Inorg. Chem.* **2004**, 2301.

(22) Blake, A. J.; Gould, R. O.; Li, W. S.; Lippolis, V.; Parson, S.; Radek, C.; Schröder, M. *Inorg. Chem.* **1998**, *37*, 5070.

(23) (a) Blake, A. J.; Li, W. S.; Lippolis, V.; Schröder, M. *Chem. Commun.* **1997**, 1943. (b) Blake, A. J.; Li, W. S.; Lippolis, V.; Taylor, A.; Schröder, M. *J. Chem. Soc., Dalton Trans.* **1998**, 2931.

(24) Küppers, H.-J.; Wieghardt, K.; Tsay, Y.-H.; Krüger, C.; Nuber, B.; Weiss, J. *Angew. Chem., Int. Ed. Engl.* **1987**, *26*, 575.

(25) Blake, A. J.; Donamaría, R.; Fernández, E. J.; Lasanta, T.; Lippolis, V.; López-de-Luzuriaga, J. M.; Manso, E.; Monge, M.; Olmos, M. E. *Dalton Trans.* **2013**, *42*, 11559.

(26) (a) Olmos, M. E.; Schier, A.; Schmidbaur, H. *Z. Naturforsch.* **1997**, *52b*, 203. (b) Barreiro, E.; Casas, J. C.; Couce, M. D.; Laguna, A.; López-de-Luzuriaga, J. M.; Monge, M.; Sánchez, A.; Sordo, J.; Varela, J. M.; Vázquez López, E. M. *Eur. J. Inorg. Chem.* **2011**, 1322.

(27) (a) Blake, A. J.; Champness, N. R.; Howdle, S. M.; Morley, K. S.; Webb, P. B.; Wilson, C. *CrystEngComm* **2002**, *4*, 88. (b) Yamaguchi, T.; Yamazaki, F.; Ito, T. *Acta Crystallogr.* **2002**, *C58*, m213. (c) Blower, P. J.; Clarkson, J. A.; Rawle, C. R.; Hartman, J. R.; Wolf, R. E., Jr.;

Yagbasan, R.; Bott, S. G.; Cooper, S. R. *Inorg. Chem.* **1989**, *28*, 4040. (d) Clarkson, J.; Yagbasan, R.; Blower, P. J.; Rawle, S. C.; Cooper, S. R. *J. Chem. Soc., Chem. Commun.* **1987**, 950.
(28) (a) Fernández, E. J.; Laguna, A.; López-de-Luzuriaga, J. M.; Olmos, M. E.; Puelles, R. C. *Z. Naturforsch.* **2009**, *64b*, 1500. (b) Lasanta, T.; Olmos, M. E.; Laguna, A.; López-de-Luzuriaga, J. M.; Naumov, P. *J. Am. Chem. Soc.* **2011**, *133*, 16358.
(29) Contel, M.; Jiménez, J.; Jones, P. G.; Laguna, A.; Laguna, M. *J. Chem. Soc., Dalton Trans.* **1994**, 2515.
(30) Addison, A. W.; Rao, T. N.; Reedijk, J.; van Rijn, J.; Verschoor, G. C. *J. Chem. Soc., Dalton Trans.* **1984**, 1349.
(31) Larson, L. J.; McMacauley, E. M.; Weissbart, B.; Tinti, D. J. *J. Phys. Chem.* **1995**, *99*, 7218.
(32) Fernández, E. J.; López-de-Luzuriaga, J. M.; Monge, M.; Montiel, M.; Olmos, M. E.; Pérez, J.; Laguna, A.; Mendizabal, F.; Mohamed, A. A.; Fackler, J. P., Jr. *Inorg. Chem.* **2004**, *43*, 3573.
(33) Pretsch, E.; Bühlmann, P.; Affolter, C.; Herrera, A.; Martínez, R. In *Structure Determination of Organic Compounds;* Springer-Verlag: Berlin, Heidelberg, New York, 2000.
(34) Fernández, E. J.; Hardracre, H.; Laguna, A.; Lagunas, M. C.; López-de-Luzuriaga, J. M.; Monge, M.; Montiel, M.; Olmos, M. E.; Puelles, R. C.; Sánchez-Forcada, E. *Chem.—Eur. J.* **2009**, *15*, 6222.
(35) Forward, J. M.; Fackler, J. P., Jr.; Assefa, Z. Photochemical Properties of Gold(I) Complexes. In *Optoelectronic Properties of Inorganic Compounds;* Roundhill, D. M., Fackler, J. P., Jr., Eds.; Plenum Press: New York, 1999; p 195.
(36) Sheldrick, G. M. *SHELXL97, Program for Crystal Structure Refinement;* University of Göttingen: Germany, 1997.
(37) Frisch, M. J.; Trucks, G. W.; Schlegel, H. B.; Scuseria, G. E.; Robb, M. A.; Cheeseman, J. R.; Scalmani, G.; Barone, V.; Mennucci, B.; Petersson, G. A.; Nakatsuji, H.; Caricato, M.; Li, X.; Hratchian, H. P.; Izmaylov, A. F.; Bloino, J.; Zheng, G.; Sonnenberg, J. L.; Hada, M.; Ehara, M.; Toyota, K.; Fukuda, R.; Hasegawa, J.; Ishida, M.; Nakajima, T.; Honda, Y.; Kitao, O.; Nakai, H.; Vreven, T.; Montgomery, J. A., Jr.; Peralta, J. E.; Ogliaro, F.; Bearpark, M.; Heyd, J. J.; Brothers, E.; Kudin, K. N.; Staroverov, V. N.; Kobayashi, R.; Normand, J.; Raghavachari, K.; Rendell, A.; Burant, J. C.; Iyengar, S. S.; Tomasi, J.; Cossi, M.; Rega, N.; Millam, N. J.; Klene, M.; Knox, J. E.; Cross, J. B.; Bakken, V.; Adamo, C.; Jaramillo, J.; Gomperts, R.; Stratmann, R. E.; Yazyev, O.; Austin, A. J.; Cammi, R.; Pomelli, C.; Ochterski, J. W.; Martin, R. L.; Morokuma, K.; Zakrzewski, V. G.; Voth, G. A.; Salvador, P.; Dannenberg, J. J.; Dapprich, S.; Daniels, A. D.; Farkas, Ö.; Foresman, J. B.; Ortiz, J. V.; Cioslowski, J.; Fox, D. J. *Gaussian 09, Revision A.1;* Gaussian, Inc.: Wallingford, CT, 2009.
(38) Adamo, C.; Barone, V. *J. Chem. Phys.* **1999**, *110*, 6158.
(39) Andrae, D.; Haeussermann, U.; Dolg, M.; Stoll, H.; Preuss, H. *Theor. Chim. Acta* **1990**, *77*, 123.
(40) Bergner, A.; Dolg, M.; Küchle, W.; Stoll, H.; Preuss, H. *Mol. Phys.* **1993**, *80*, 1431.
(41) Huzinaga, S. *Gaussian Basis Sets for Molecular Calculations;* Elsevier: Amsterdam, 1984; p16.
(42) Huzinaga, S. *J. Chem. Phys.* **1965**, *42*, 1293.
(43) Gorelsky,S. I. *AOMix: Program for Molecular Orbital Analysis.* http://www.sg-chem.net/, version 6.87, 2013.
(44) Gorelsky, S. I.; Lever, A. B. P. *J. Organomet. Chem.* **2001**, *635*, 187.
(45) Ros, P.; Schuit, G. C. A. *Theor. Chim. Acta (Berlin)* **1966**, *4*, 1.